CHARLES UNIVERSITY IN PRAGUE
Faculty of Physical Education and Sport

Influence of Temperature and Stimulus Intensity on FAD Transience in Rat Hippocampal Slices in Vitro

DIPLOMA THESIS

Author: Matouš Rous
Supervisor: MUDr. Jakub Otáhal, Ph.D.

Prague, September 2008

UNIVERZITA KARLOVA V PRAZE
Fakulta tělesné výchovy a sportu

Vliv teploty a intenzity stimulace na FAD autofluorescenci u hipokampálního řezu potkana in vitro

DIPLOMOVÁ PRÁCE

Autor: Matouš Rous
Vedoucí diplomové práce: MUDr. Jakub Otáhal, Ph.D.

Praha, září 2008

SUMMARY

Title:

Influence of temperature and stimulus intensity on FAD transience in rat hippocampal slices in vivo.

Aims:

The purpose of this study was to characterize the influence of temperature and stimulus intensity on flavoprotein autofluorescence in rat hippocampal slices.

Methods:

Experiments were performed in hippocampal slices of adult male Wistar rats. Slices of 400 μm of thickness were maintained in submerged recording chamber, through which oxygenated ACSF was perfused (2 ml/min). Synaptic activation was being made by bipolar stimulating electrode (10s stimulus train 20Hz) placed in hillus of the dentate gyrus (Mossy fibers). FAD signals were detected by cooled 12-bit CCD-camera (RETIGA2000R).

Results:

Our findings demonstrate that FAD autofluorescence signals were significantly decreased at higher temperature. The data confirmed that FAD autofluorescence signals showed smaller light intensity in different layers of CA3 under the same conditions at 36°C compared to 26°C.

Our data approved that under defined conditions FAD fluorescence signals have risen during stimulation.

Keywords:

Mitochondria, FAD autofluorescence, temperature, stimulus intensity, hippocampus, rat.

SOUHRN

Název:

Vliv teploty a intenzity stimulace na FAD autofluorescenci u hipokampálního řezu potkana in vitro.

Cíle práce:

Charakterizovat vliv teploty a intenzity stimulace na FAD autofluorescenci u hipokampálního řezu potkana in vitro.

Metody:

Experimentální studie proběhla na dospělých samčích laboratorních potkanech Wistar. Řezy tloušťky 400 um byly ponořeny v záznamové komůrce, kterou protékal okysličený umělý mozkomíšní mok (2ml/min). Synaptická aktivace byla vyvolávána bipolární stimulační elektrodou (10s stimulačním proudem 20Hz) umístěnou v hilu gyrus dentatus (v mechových vláknech). FAD signály byly detekovány pomocí 12-bit CCD-camery (RETIGA2000R).

Výsledky:

Výsledky demonstrují, že FAD autofluorescence byla signifikantně nižší při vyšší teplotě. Data potvrdila, že autofluorescence byla nižší v různých vrstvách CA3 hipokampu při teplotě 36°C než při teplotě 26°C.

Data také dokládají, že se při stejných laboratorních podmínkách FAD fluorescence během stimulace zvyšuje.

Klíčová slova:

Mitochondrie, FAD fluorescence, teplota, intenzita stimulace, hipokampus, potkan.

ACKNOWLEDGMENTS

In the first place, I would like to express my gratitude to Mgr. Renata Konopková, who was abundantly helpful and offered invaluable assistance, support and guidance.

I am also grateful to my supervisor MUDr. Jakub Otáhal, Ph.D. for his relevant and erudite comments on my work.

Thanks belong to the all the members of the Department of developmental epileptology for creating a pleasant working atmosphere.

The work on this project was carried out at the Academy of Science of the Czech Republic.

This diploma thesis was supported by the grant of the Academy of Sciences of the Czech Republic (No. 1QS501210509).

Prague, 5.9.2008 Matouš Rous

.....

Prohlašuji, že jsem diplomovou práci zpracoval samostatně a použil jsem pouze literaturu uvedenou v seznamu bibliografické citace.

V Praze 5.9.2008 Matouš Rous

.....

Souhlasím se zapůjčením práce ke studijním účelům. Prosím, aby byla vedena přesná evidence vypůjčovatelů, kteří musí pramen převzaté literatury řádně citovat.

Jméno a příjmení Datum

Poznámka

CONTENTS

1. INTRODUCTION

Every cell of human organism needs energy for its live. The universal carrier of energy in cell is adenosinetriphosphate (ATP), which major consumption in the central nervous system is thought to be generated by oxidative metabolism within mitochondria. (19) The integrity of mitochondrial function is therefore fundamental to cell life. Disturbances of mitochondrial function will lead to the disruption of cell function which can be expressed as a disease or even death. (37)

Indeed, mitochondria lie at the heart of cell life and cell death. In order to their function our mitochondria demand oxygen. 98% or so of the oxygen that we breathe is destined to be consumed by our mitochondria. (19) Without mitochondria, oxygen would be of no use to us, we would not even need the oxygen transfer machinery of the lungs. There would be no need for erytrocytes, or haemoglobin, or even for the complexity of a circulatory system to deliver oxygen to the tissues. Mitochondria are essential to maintain the battle against entropy that is necessary to sustain life. They provide the energy required for almost all cellular processes – to allow muscle to contract – that includes skeletal, cardiac and smooth muscle. They are required to provide energy to maintain ionic gradients across cell membranes which is necessary for the flexibility of excitable cells, such as neurons. In the following chapters we should consider that neurons are very vulnerable to anoxia, luck of energy.

Restricted mitochondrial function can be found during the reperfusion of ischaemic heart, brain and kidney; mutations of mitochondrial proteins gives rise to a range of ill understood patterns of disease; mitochondrial dysfunction has been implicated in all the major neurodegenerative diseases - Parkinson's, Alzheimer's, motor neuron disease (Lou-Gehrig's disease or Amyotrophic Lateral sclerosis) and possibly in Multiple Sclerosis. Mitochondrial dysfunction may give rise to myopathy of various types. Mitochondrial function is central to

transduction in the pancreatic beta cell and the secretion of insulin in response to glucose, and so dysfunction gives rise to diabetes. Most recently evidence points to a major role for mitochondrial dysfunction in the condition of multi-organ system failure in sepsis.

Accumulations in mitochondrial defects have been implicated as a mechanism of ageing and age related disease. Indeed, the production of free radicals by mitochondria has been considered by many as a key in the cellular injury that appears to underlie the process of ageing, while interestingly some of the genes identified in the control of longevity appear to target mitochondria or at least to alter antioxidant defences of the cell.

Over the last few years, the central role of mitochondria in the regulation of organized or programmed 'apoptotic' cell death has been a revelation. The centrality of apoptosis in development and in disease is extraordinary. If the process of apoptosis is activated inappropriately it will lead to tissue dysfunction and damage, and if it fails to be activated when necessary, cancers are the result, making this whole area absolutely critical in understanding the role of mitochondria in disease.

As noted, mitochondria and mitochondrial dysfunction have been implicated in many different aspects of health and disease. Understanding of complex interactions between mitochondria and other aspects of cell function in pathophysiological states requires as full general understanding of all aspects of mitochondrial biology as possible. In my diploma thesis, I have tried to take a part in the process and have tried to show how the temperature influence mitochondrial energy demands during electrophysiogical stimulation in rat hippocampal slices using flavinadenindinucleotide (FAD) autofluorescence signals.

2. THEORETICAL BACKGROUND

2.1. RAT HIPPOCAMPUS

Before discussing the aspects of cellular metabolism impairment in rat hippocampal slices, it is useful to review the relevant hippocampal anatomy. There is a brief summary emphasizing the characteristics that are thought to be important for the hippocampus's unique physiological properties that make hippocampus a useful model for the study of properties of central nervous system (CNS). Except where noted, the following description is based on Amaral and Witter. (1)

In the rat, the hippocampal formation is a relatively large structure, its surface area rivaling that of the entire isocortex. The bilateral hippocampal formation appears similar to the curved horns of a ram, hence its early name "*Cornu Ammonis*" (Ammon's horn), after which its CA1-3 fields are named. Each roughly C-shaped side extends from the septal nuclei dorsally and caudally over the diencephalon, and then ventrally and rostrally tucks under the temporal lobe (Fig. 1.1). For more detailed diagram of the rat hippocampus see Att. 1.

The hippocampal formation includes the **entorhinal cortex (EC)**; **dentate gyrus (DG)**; **hippocampus proper**, which is subdivided into fields CA1, CA2, and CA3 (although the existence of CA2 in the rat is controversial and rarely mentioned in the physiology literature); and the **subicular complex**, consisting of the subiculum, presubiculum, and parasubiculum.

Dentate gyrus (DG) contains three layers, **molecular layer** (contains dendrites of granule cells, basket and polymorphic cell, axonal arbors); the **granule cell layer (principal cell layer)** which is made up primarily of densely packed columnar stacks of granule cells; **the polymorphic cell layer (mossy cells)**.

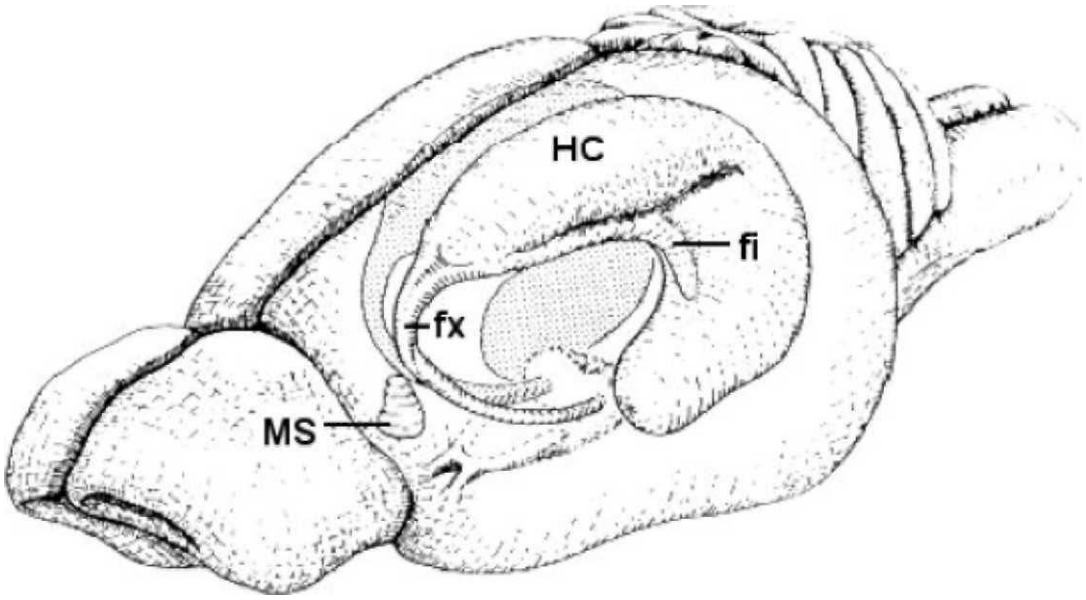

Figure 1.1: *Layout of hippocampus in rat brain.*
Left is anterior, right is posterior. Abbreviations: HC = hippocampus; fx = fornix; MS = medial septum; fi = fimbria.

The major intrinsic hippocampal connections are summarized schematically in Figure 1.2. The EC, which has strong projections to and from most areas of neocortex except primary sensory areas, provides the sole cortical input and major cortical output of the hippocampal formation (CA1 and subiculum also project directly to some cortical areas, bypassing the EC). The superficial layers of the EC project to all the other fields of the hippocampal formation via the "perforant path": EC layer 2 projects primarily to the dentate gyrus and CA3, and EC layer 3 projects primarily to CA1 and the subiculum. In addition, the granule cells of the DG project to CA3 as the "**mossy fibers**"; CA3 contains extensive recurrent collaterals, such that the primary input of its projection cells (pyramidal cells) are other CA3 pyramidal cells; CA3 pyramidal cells project to CA1 as the "**Schaffer collaterals**"; and CA1 pyramidal cells project to the subiculum. The deep layers (4-6) of the EC receive hippocampal output via the subiculum and CA1. Also, DG granule cells project to the contralateral DG, and CA3 and perhaps some CA1 pyramidal cells project to the contralateral CA3,

CA2, and CA1, as the associational/commissural fibers. All of the aforementioned projections are glutamatergic.

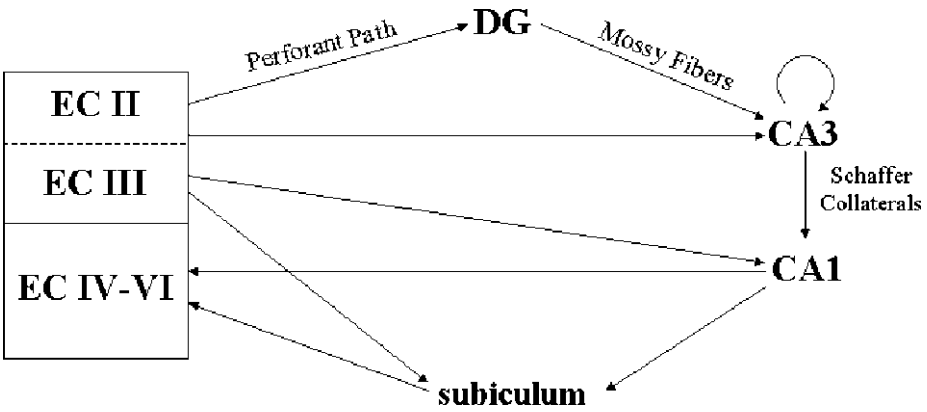

Figure 1.2. *Major intrinsic connections of the hippocampal formation.*
Abbreviations: EC = entorhinal cortex; DG = dentate gyrus; INs = interneurons.

The hippocampal formation also has interconnections with subcortical structures, primarily coursing through the fimbria/fornix.

The cross-section of the hippocampal formation has a striking laminar profile. Each field (DG, CA1, and CA3) contains a thin plane of projection cell bodies, granule cells in the DG and **pyramidal cells** in fields CA1-3. The anatomical layout of these principal cell layers and a subset of their intrahippocampal projections, the classical "**trisynaptic circuit**" (2), are shown schematically in Figure 1.3. All of the projection cells are neatly aligned with their apical dendrites extending toward the hippocampal fissure (the division between the dentate gyrus and CA1) and the basal dendrites and axons extending toward the outer surface of the hippocampus.

In the DG, as noted above, there are 2 other layers, the molecular layer, which is closest to the hippocampal fissure, and the polymorphic layer, more often called the **hilus**, on the other side of the granule cell layer, closest to CA3. In the CA fields, the narrow, cell-free layer just deep to the pyramidal cell layer is called *stratum oriens*, in which most of the basal dendritic tree is located, and

deep to this is the fiber-containing **alveus**. In the CA3 field, but not in CA2 or CA1, there is a narrow layer called the *stratum lucidum*, containing the mossy fiber projections from the dentate gyrus. Just above the pyramidal cell layer in CA2 and CA1, and just above the stratum lucidum in CA3, is the *stratum radiatum*, in which the CA3 recurrent collaterals and CA3-CA1 Schaffer collaterals are located. The most superficial (i.e. closest to the hippocampal fissure) layer is the *stratum lacunosum-moleculare*, in which perforant pathway fibers from the EC travel and terminate. In addition to the projection cells, each layer of each field also contains a heterogeneous mix of interneurons, the vast majority of which are GABAergic. The interneurons receive inputs from the same regions as the principal cells in that field, and they also project to and receive inputs from the local principal cells. They are predominantly local circuit neurons, but some are also known to project outside their subfields.

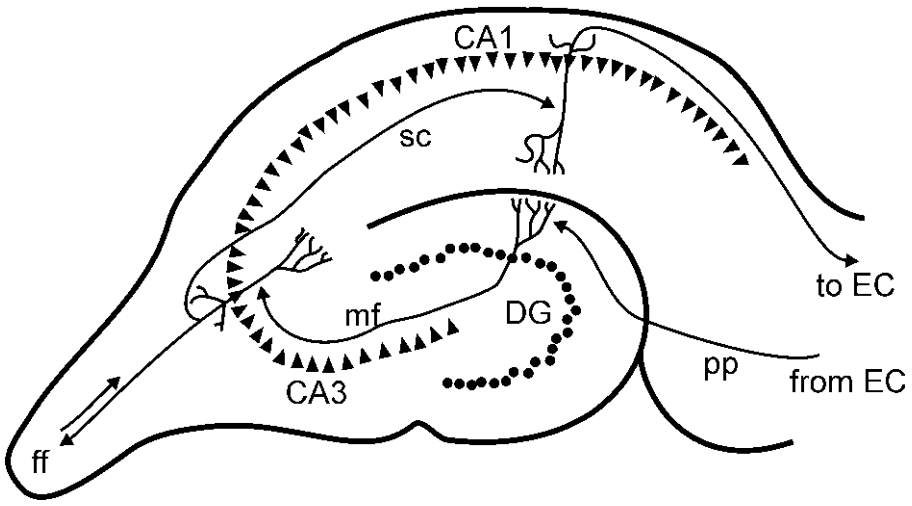

Figure 1.3. *Cross-section of hippocampus.*
This schematic of the coronal cross-section of dorsal hippocampus illustrates the layout of the principal cell layers of DG, CA3, and CA1. It also illustrates the layout of a subset of the intrinsic outputs of these principal cells, known classically as the "trisynaptic circuit" (2): EC to DG (synapse 1), DG to CA3 (synapse 2), and CA3 to CA1 (synapse 3). The projections from CA1 back to EC are also shown. It is now known that the projections through the hippocampus, although still primarily feed-forward, are more elaborate than this (see text). Abbreviations: EC = entorhinal cortex; DG = dentate gyrus; pp = perforant pathway; mf = mossy fibers; sc = Schaffer collaterals; ff = fimbria/fornix.

2.2. THE NEURON

As I was measuring autofluorescence in neuronal slices of a rat, I would like to show some basics of neuronal morphology and functioning. There are of course other cells in the slices – glial cells (neroglia) including oligodendrocytes, astrocytes and microglia; vascular cells etc. but the main changes in autoflostescence of the tissue are thought to have resulted from neuronal metabolic processes before, during and after electrical train stimulation. I will therefore focus on neurons. Except where noted, the following description is based on Ganong. (27)

2.2.1. MORPHOLOGY

Neurons in the rat nervous system as well as in all mammals come in many different shapes and sizes. However, most have the same parts as the typical spinal motor neuron (see Fig. 2.1). This cell has five to seven processes called **dendrites** that extend outward from the cell body and arborize extensively. Particularly in the cerebral and cerebellar cortex, the dendrites have small knobby projections called **dendritic spines**. A typical neuron has also a long fibrous **axon** that originates from a thickened area of the cell body, the **axon hillock**. The first portion of the axon is called the **initial segment**. The axon divides into terminal braches, each ending in a number of **synaptic knobs**. The knobs are also called **terminal buttons** or **axon telodendria**. They contain granules or vesicles in which the transmitters secreted by the nerves are stored.

The axons of many neurons are myelinated, that is, they acquire a sheath of **myelin**, a protein-lipid complex that is wrapped around the axon. In the CNS of mammals, most neurons are myelinated by oligodendrocytes while outside the CNS, the myelin is produced by Schwann cells, glia-like cells found along the axon. The myelin sheath envelops the axon except at its ending and at the

nodes of Ranvier, periodic 1-μm constrictions that are about 1mm apart. The insulating function of myelin is to support the fast nerve conduction described as **salutatory conduction**. Unlike the Schwann cell, which forms the myelin between two nodes of Ranvier on a single neuron, oligodendrocytes send off multiple processes that form myelin on many neighboring axons. In multiple sclerosis a crippling autoimmune disease, patchy destruction of myelin occurs in the CNS. The loss of myelin is associated with delayed or blocked conduction in the demyelinated axons. But not all mammalian neurons are myelinated. Some are unmyelinated; simply surrounded by other cells without the wrapping of the oligodendrocyte or Schwann cell membrane around the axon that produces myelin.

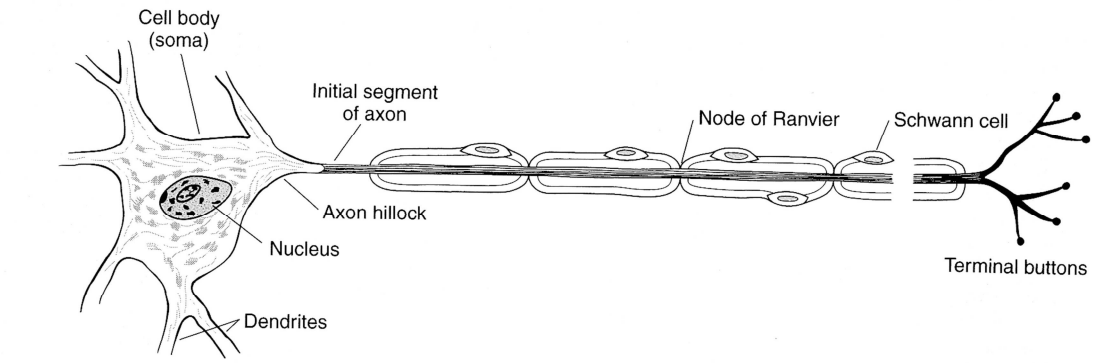

Figure 2.1. *Motor neuron with myelinated axon.*

Glia and non-neuroglia elements make up almost 70% of the volume of the neocortex. Of the remainder, 22% consists of axons and dendrites, with the body (soma) of the neuron comprising only 8%. (76)

The neocortex can vary in thickness and topology. In comparison of the human and rat cortices we can see a definite difference in shape. The wave like nature of the cortex we see in the human brain is not as apparent in the brain of the rat. (9)

The cortex structure is highly folded with many grooves (called 'sulci'). This folded arrangement allows for a far greater volume of cortical matter to be contained within a given-sized brain cavity than would be possible if the cortex were laid out in a 'sheet' directly beneath the skull. The sulci provide convenient 'landmarks' for helping anatomists to classify different regions of the cerebral cortex. (96) The defined areas of the cortex include the motor cortex, the sensory cortex and the associative cortex. All three of theses areas are responsible for functions of the organisms ranging from control of body movement to sound recognition to mental processing. (9)

2.2.2. RESTING MEMBRANE POTENTIAL

When two electrodes are placed on the surface of a single axon, no potential difference is observed. However, if one electrode is inserted into the interior of the neuron, a constant potential difference is observed, with the inside negative relative to the outside of the cell at rest. This resting membrane potential is found in almost all cells. Its genesis is discussed below. In neurons, it is usually about -70 mV.

2.2.3. GENESIS OF RESTING MEMBRANE POTENTIAL

The distribution of ions across the cell membrane and the nature of this membrane provide the explanation for the resting membrane potential. The intracellular and extracellular concentration of potassium (K^+) and natrium (Na^+) ions play the major role in this process. The concentration gradient for K^+ facilitates its movement out of the cell via K^+ channels, but its electrical gradient is in the opposite (inward) direction. Consequently, an equilibrium is reached in which the tendency of K^+ to move out of the cell is balanced by its tendency to move into the cell, and at that equilibrium there is a slight excess of cations on the outside and anions on the inside. This condition is maintained

by Na^+-K^+ATPase, which pumps K^+ back into the cell and keeps the intracellular concentration of Na^+ low. The Na^+-K^+ pump is also electrogenic, because it pumps three Na^+ out of the cell for every two K^+ it pumps in; thus, it also contributes a small amount to the membrane potential by itself. It should be emphasized that the number of ions responsible for the membrane potential is a minute fraction of the total number present and that the total concentrations of positive and negative ions are equal everywhere except along the membrane. Na^+ influx does not compensate for the K^+ efflux because the K^+ channels make the membrane more permeable to K^+ than to Na^+. As a result of this, there is the resting membrane potential with the inside negative relative to the outside of the neuron

2.2.4. EXCITATION AND CONDUCTION

Neurons have probably evolved from primitive neuroeffector cells that responded to various stimuli by contracting. In more complex organisms, contraction has become the specialized function of muscle cells, whereas integration and transmission of nerve impulses have become the specialized function of neurons.

Nerve cells have a low threshold for excitation. The stimulus may be electrical, chemical, or mechanical. Two types of physicochemical disturbances are produced: local, nonpropagated potentials called, depending on their location, **synaptic**, **generator**, or **electrotonic potentials**; and propagated disturbances, the **action potentials** (or **nerve impulses**). These are the only electrical responses of neurons and other excitable tissues, and they are the main language of the nervous system. They are due to changes in the conduction of ions across the cell membrane that are produced by alterations in ion channels.

The impulse is normally transmitted (**conducted**) along the axon to its termination. Nerves are not "telephone wires" that transmit impulses passively;

conduction of nerve impulses, although rapid, is much slower than that of electricity. Nerve tissue is in fact a relatively poor passive conductor, and it would take a potential of many volts to produce a signal of a fraction of a volt at the other end of a meter-long axon in the absence of active processes in the nerve. Conduction is an active, self-propagating process, and the impulse moves along the nerve at a constant amplitude and velocity. The electrical events in neurons are rapid, being measured in **milliseconds (ms)**; and the potential changes are small, being measured in **millivolts (mV)**.

2.2.5. ACTION POTENTIAL

If the axon is stimulated and a conducted impulse occurs, a characteristic series of potential changes known as the **action potential** is observed as the impulse passes the external electrode (see Fig. 2.2). It is monophasic because one electrode is inside the cell.

When the stimulus is applied, the **stimulus artifact**, a brief irregular deflection of the baseline, occurs. This artifact is due to current leakage from the stimulating electrodes to the recording electrodes. It usually occurs despite careful shielding, but it is of value because it marks on the cathode ray screen the point at which the stimulus was applied.

The stimulus artifact is followed by an isopotential interval (**latent period**) that ends with the start of the action potential and corresponds to the time it takes the impulse to travel along the axon from the site of stimulation to the recording electrodes. Its duration is proportionate to the distance between the stimulating and recording electrodes and inversely proportionate to the speed of conduction.

The first manifestation of the approaching action potential is a beginning depolarization of the membrane. After an initial 15 mV of depolarization, the rate of depolarization increases. The point at which this change in rate occurs is

called the **firing level** or sometimes the **threshold**. Thereafter, the curve (tracing on the oscilloscope) rapidly reaches and overshoots the isopotential (zero potential) line to approximately +35 mV. It then reverses and falls rapidly toward the resting level. When repolarization is about 70% completed, the rate of repolarization decreases and the curve approaches the resting level more slowly. The sharp rise and rapid fall are the spike **potential** of the neuron, and the slower fall at the end of the process is the **after-depolarization**. After reaching the previous resting level, the tracing overshoots slightly in the hyperpolarizing direction to form the small but prolonged **after-hyperpolarization**.

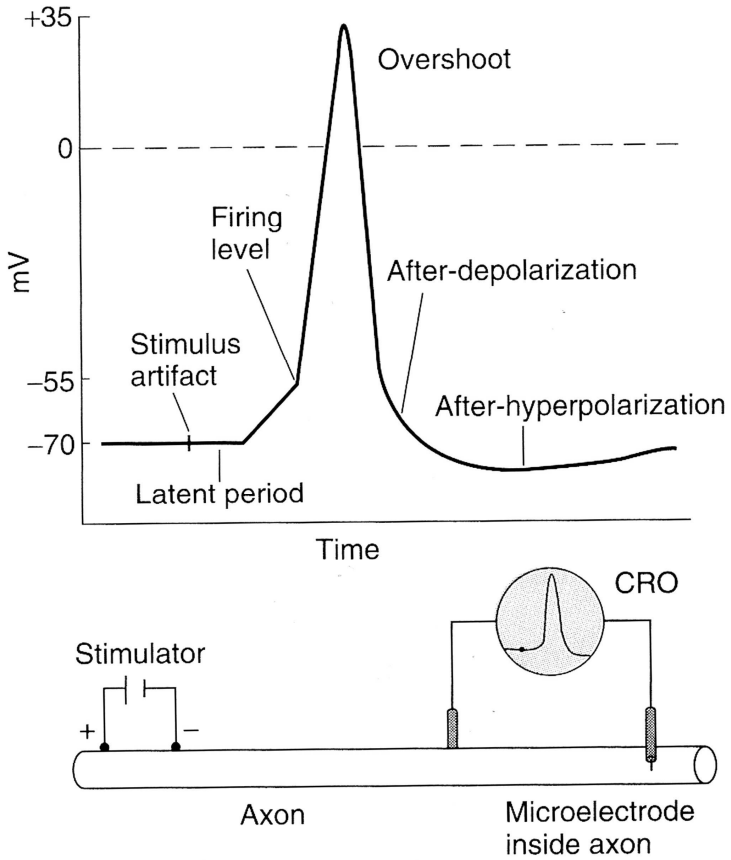

Figure 2.2: *Action potential in a neuron recorded with one electrode inside the cell.*

Action potentials are all-or-none events and neurons act under so called **all-or-none law**. It means that any stimulus large enough to produce an action potential produces the same size action potential, regardless of the stimulus strength. In other words, once the stimulus is above threshold, the amplitude of the response no longer reflects the amplitude of the stimulus. (45)

2.2.6. IONIC BASIS OF EXCITATION AND CONDUCTION

The cell membranes of nerves, like those of other cells, contain many different types of ion channels. Some of these are voltage-gated and others are ligand-gated. It is the behavior of these channels, and particularly Na^+ and K^+ channels, that explains the electrical events in nerves. It has been described above that K^+ channels maintain the resting membrane potential.

The changes in membrane conductance of Na^+ and K^+ that occur during the action potentials are shown in Figure 2.3. The conductance of an ion is the reciprocal of its electrical resistance in the membrane and is a measure of the membrane permeability to that ion.

When the firing level is reached, the voltage-activated Na^+ channels overwhelm the K^+ and other channels and the spike potential results. The equilibrium potential for Na^+ in mammalian neurons is about +60 mV. The membrane potential moves toward this value but does not reach it during the action potential, primarily because the increase in Na^+ conductance is short-lived. The Na^+ channels rapidly enter a closed state called the **inactivated state** and remain in this state for a few milliseconds before returning to the resting state. In addition, the direction of the electrical gradient for Na^+ is reversed during the overshoot because the membrane potential is reversed, and this limits Na^+ influx. A third factor producing repolarization is the opening of voltage-gated K^+ channels. This opening is slower and more prolonged than the opening of the Na^+ channels, and consequently, much of the increase in K^+ conductance comes after the increase in Na^+ conductance. This helps complete the process

of repolarization. The slow return of the K^+ channels to the closed state also explains the after-hyperpolarization.

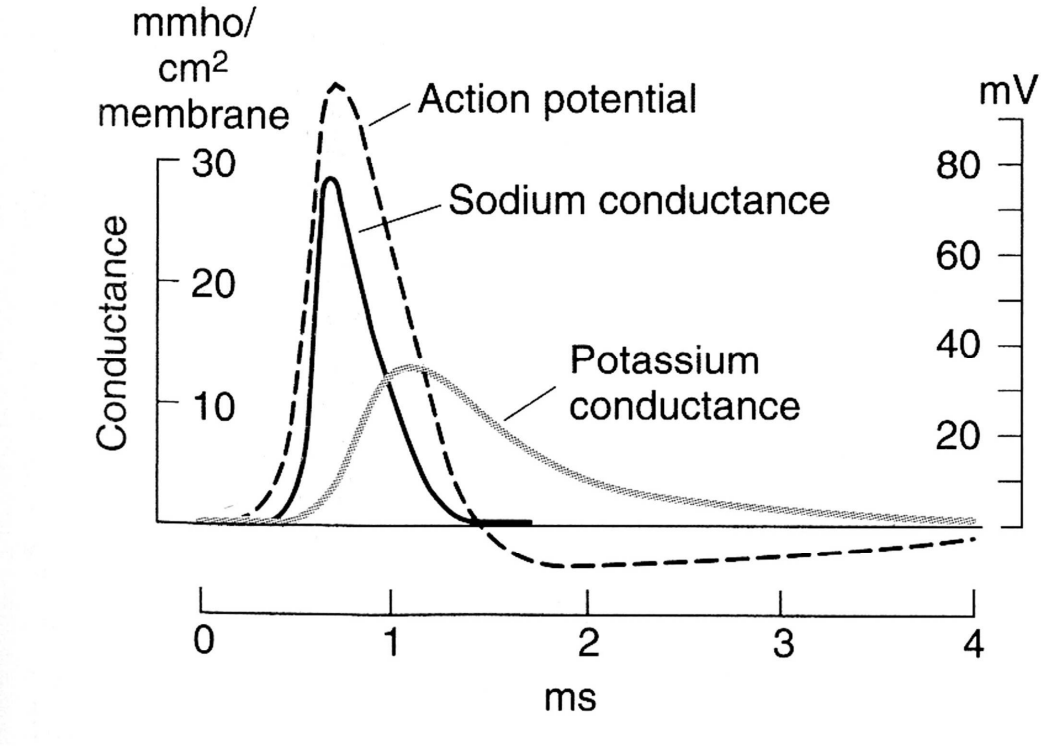

Figure 2.2: *Changes in Na+ and K+ conductance during the action potential in giant squid axon.* The dashed line represents the action potential superimposed on the same time coordinate.

Decreasing the external Na^+ concentration decreases the size of the action potential but has little effect on the resting membrane potential. The lack of much effect on the resting membrane potential would be predicted, since the permeability of the membrane to Na^+ at rest is relatively low. Conversely, increasing the external K^+ concentration decreases the resting membrane potential.

The slower opening and delayed closing of the voltage-gated K^+ channels also explain accommodation. If depolarization occurs rapidly, the opening of the Na^+ channels overwhelms the repolarizing forces, but if the induced depolarization is

produced slowly, the opening of K^+ channels balances the gradual opening of Na^+ channels, and an action potential does not occur.

A decrease in extracellular Ca^{2+} concentration increases the excitability of nerve and muscle cells by decreasing the amount of depolarization necessary to initiate the changes in the Na^+ and K^+ conductance that produce the action potential. Conversely, an increase in extracellular Ca^{2+} concentration "stabilizes the membrane" by decreasing excitability.

2.3. THE MITOCHONDRION

2.3.1. EVOLUTIONARY HISTORY

The mitochondrion as well as the chloroplast is thought to have evolved from a bacterial progenitor around the same time and in much the same way. It is probably no exaggeration to suggest that this evolutionary step has been crucial for all sophisticated life forms - the chloroplast harnessing energy from the sun to generate oxidiseable fuels, and the mitochondrion to use those fuels to generate energy rich biochemical compounds.

2.3.2. STRUCTURE

Mitochondria are defined by two membrane systems, the inner and outer mitochondrial membrane. Occasionally these membranes come together to form junctional complexes or contact sites. The outer mitochondrial membrane is relatively permeable to small molecules and ionic species while the inner mitochondrial membrane is largely impermeable and forms the major barrier between the cytosol and the mitochondrial matrix. The space between the two membranes is described as the intermembrane space, recently revealed as an interesting microenvironment of which we understand little, but housing some

proteins which play major roles in cell physiology, particularly mitochondrial energetics and in cell death - perhaps cytochrome c and creatine kinase.

The inner mitochondrial membrane forms multiple infoldings called cristae which house a variety of mitochondrial membrane bound enzymes systems. The structure of cristae varies enormously between cell types. In brown fat cell mitochondria appear tightly packed with lamellar cristae, while steroid synthesising cell has cristae that seem to form tubular networks. Several groups of scientists have tried to show detailed three-dimensional reconstructions of cristae structure and to model the bioenergetic consequences of changing shapes of cristae. (25, 33, 51, 52, 17, 26)

Mitochondrial features of their more 'macroscopic' structures also vary between tissues. In some tissues mitochondria clearly form complex highly mobile interconnecting networks while they seem to exist as more structurally discrete and independent structures in other tissues. There is no doubt that this is due to the functional differences that have not yet been explored adequately. It has been suggested that mitochondrial networks may form a compartment in which contents and membranes are constantly interchanging, so that perhaps it would be misleading to talk of 'a mitochondrion'. However, most of the research has been done on cell lines maintained in culture. Even within different primary cells in culture or freshly isolated cells, mitochondria differ between cell types. Perhaps mitochondria even differ between cells at different stages of the cell cycle. Perhaps those differences might even follow functionally important responses of different tissues to toxic processes.

In fact, even within single cells mitochondrial heterogeneity could be seen - in skeletal and also in cardiac muscle, mitochondria could be divided into two pools, the **interfibrillar** mitochondria and the **subsarcolemmal** mitochondria. The interfibrillar ones are dense in electron micrographs whilst the subsarcolemmal are paler, lighter and situated underneath the plasma membrane. These two classes of mitochondria require different procedures to

isolate them and purified preparations of mitochondria contain two classes of organelle which have different biochemical properties, express different levels of enzymes, and appear to respond differently to stresses such as anoxia and reperfusion. (46) There appear to be differences in the content of respiratory enzymes. The functional significance of this differentiation as well as the physiological and pathological pathways is really not understood.

2.3.3. THE CHEMIOSMOTIC PRINCIPLE

The key enzymatic components of the mitochondria are the **citric acid** or **tricarboxylic acid (TCA) cycle** and the **respiratory** or **electron transport chain.** The enzyme system of the TCA cycle breaks down carbon substrates acetyl CoA, derived from pyruvate, fatty acid and amino acid breakdown to generate CO_2 and in the process to reduce NAD^+ to NADH and FAD^{2+} to $FADH_2$. These intermediates provide reducing equivalents to the respiratory chain which consists of a series of enzyme systems coupled together and described as Complex I, II, III and IV. Complex I, NADH dehydrogenase, Complex II succinate dehydrogenase, Complex III (ubiquinol cytochrome c reductase), and Complex IV (cytochrome c oxidase) are all complex membrane spanning enzyme systems consisting of many protein subunits. Interestingly, the proteins of Complex II are entirely encoded by the nucleus, while all the other complexes represent a mixture of proteins some encoded by nuclear DNA, some encoded by the mitochondrial DNA.

The respiratory chain converts metabolites of TCA cycle to CO_2 and water. In the process, complexes I, III, and IV pump protons (H^+) into the intermembrane space. The protons then flow through **ATP synthase**, which generates ATP (see Fig. 2.3). ATP synthase (in some literature called Complex V) is unique in that part of it rotates in the genesis of ATP.

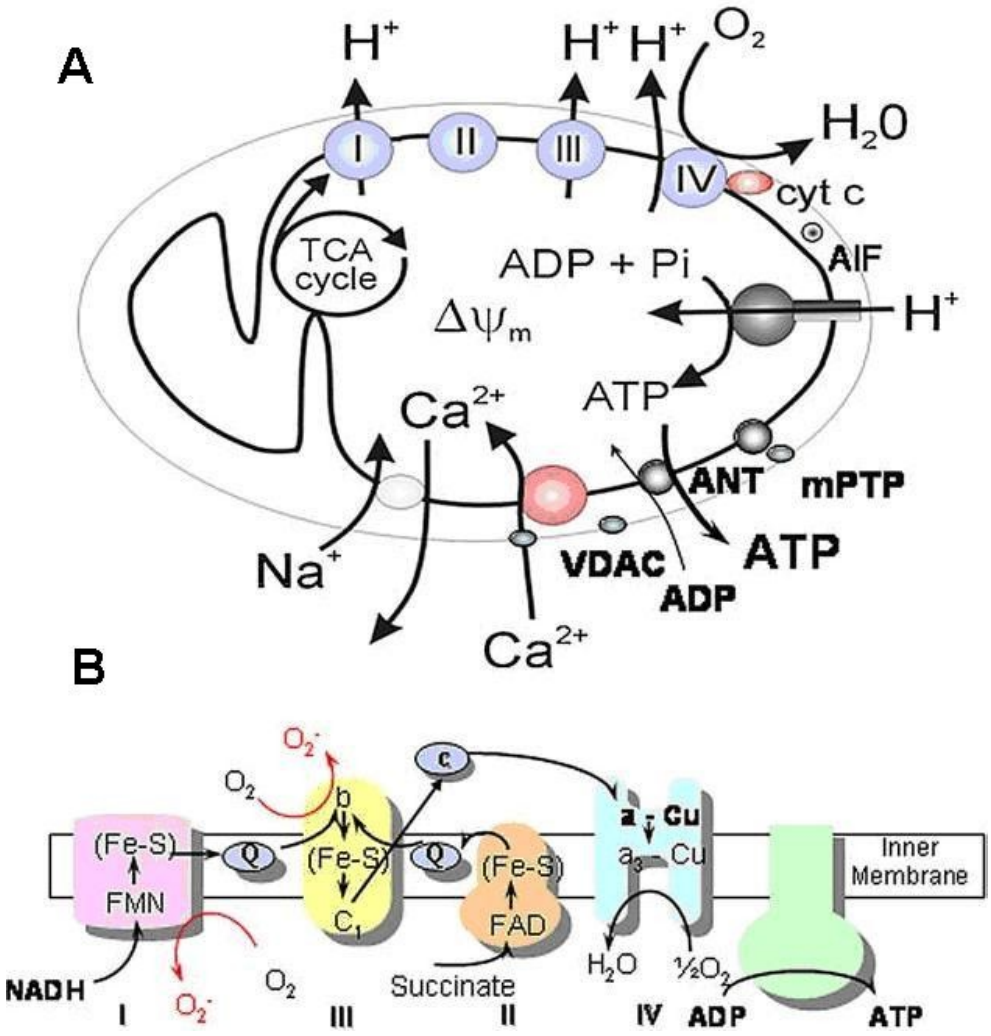

Figure 2.3: *Function of the mitochondrion.*
In (A) the functional components of the mitochondrion are shown and (B) shows a more detailed scheme of the respiratory chain.

2.3.4. MITOCHONDRIAL FUNCTION AND CELL SIGNALING

2.3.4.1. Intracellular signalization and calcium

Intracellular processes in all their complexity that we still understand very little respond to a variety of signals that could be of physical or chemical origin. If the signal is being proceed by a particular substance or molecule we call it a

messenger. The extracellular messengers are called "first messengers" and consequently the intracellular mediators are called "second messengers". I will therefore dwell on one of the most discussed "second messenger" which is calcium molecule (Ca^{2+}). It is widely agreed that Ca^{2+} regulates a very large numbers of physiologic processes that are as diverse as muscle contraction, neural signaling, learning, concentration, secretion, proliferation, and fertilization. It is also agreed that Ca^{2+} play an important role in pathophysiological processes such as necrosis and apoptosis which importance I will discuss later. Thus regulation of intracellular Ca^{2+} is of a great importance. The free Ca^{2+} concentration in the cytoplasm $[Ca^{2+}]_c$ at rest is maintained at about 100 nmol/l. The Ca^{2+} concentration in the interstitial fluid is about 12000 times the cytoplasmic concentration. As a result of this there is a marked inwardly directed concentration gradient as well as an inwardly directed electrical gradient. Finally Ca^{2+} influx or increase in $[Ca^{2+}]_c$ is thought to be the biological correlate of the cytosolic calcium signal.

2.3.4.2. Mitochondrial calcium uptake

The principle function of the mitochondrial potential is clearly to drive ATP synthesis but it also provides the major mechanism to handle calcium. In the last decade it seems ever clearer that mitochondrial calcium handling is strongly implicated in many disease processes, as the accumulation of calcium into mitochondria has major functional consequences for the mitochondria and for the cell both in terms of physiology and pathology. Most physiological calcium signals in most cells is associated with some measure of calcium accumulation in mitochondria. (75) Furthermore, it is now widely held that many of the pathological states in which mitochondrial dysfunction has been implicated may involve alterations in mitochondrial calcium handling or a pathological effect of mitochondrial calcium 'overload' (see below). It is therefore crucial to understand the basic functional machinery involved in this pathway.

Mitochondrial calcium uptake is primarily driven by the electrochemical potential gradient established by the mitochondrial membrane potential and by a relatively low intramitochondrial Ca^{2+} concentration ($[Ca^{2+}]_m$). Whenever energised mitochondria are exposed to raised $[Ca^{2+}]_c$, Ca^{2+} will move from cytosol into their matrix, driven by the electrochemical potential gradient for Ca^{2+}. Thus, Ca^{2+} movement into mitochondria depends on the mitochondrial membrane potential and also on the intramitochondrial $[Ca^{2+}]$ ($[Ca^{2+}]_m$). Typically, mitochondrial calcium uptake follows the cytosolic signal with a time lag and re-equilibration of mitochondrial calcium is relatively slow so that mitochondria may effectively seem to integrate cytosolic calcium signals over time. (33)

Ca^{2+} is taken up through the mitochondrial inner membrane by a uniporter. The biophysical properties of this pathway and its molecular identity have yet to be defined. The mitochondrial outer membrane has been assumed to be permeant to small ions and so has been largely neglected in considerations of mitochondrial Ca^{2+} handling. However, the outer membrane may play a more significant role in modulating access of Ca^{2+} to the uniporter through the selectivity filter of the voltage-dependent anion channel (VDAC). It appears that VDAC is Ca^{2+} permeant and is regulated by $[Ca^{2+}]$. (28) It points to the outer membrane as a significant permeability barrier that may itself be regulated.

2.4.4.3. Mitochondrial Ca^{2+} efflux

The major route for Ca^{2+} efflux from mitochondria is an $x Na^+/Ca^{2+}$ exchange. The stoichiometry of the exchanger seems still to be controversial. Jung et al. (36) suggested a stoichiometry of $3Na^+/Ca^{2+}$, in which case the operation of the exchanger will be dependent on mitochondrial membrane potencial. The inhibition of mitochondrial Ca^{2+} efflux by mitochondrial depolarisation supports this electrogenic stoichiometry. (6, 57)

2.4.4.4. Mitochondrial influence on resting cytosolic Ca^{2+} concentration

Many excitable cells respond to depolarisation with a rise in $[Ca^{2+}]_c$ which rises rapidly and recovers with an initial rapid phase and a slower second phase that can even form a plateau. (4, 89) It has been established that the slow recovery phase reflects the redistribution of mitochondrial Ca^{2+} through the activity of the Na^+/Ca^{2+} exchanger typically initiated at a $[Ca^{2+}]_c$ of 500 nmol/l. This particular $[Ca^{2+}]_c$ is termed the "**set point**" for mitochondrial Ca^{2+} uptake. The operation of this system has functional consequences at presynaptic terminals, where the $[Ca^{2+}]_c$ plateau that follows repetitive stimulation, maintained by the re-equilibration of mitochondrial Ca^{2+}, provides an elevated $[Ca^{2+}]_c$ baseline upon which subsequent stimulation initiates an enhanced synaptic response—the basis for post-tetanic potentiation of synaptic transmission (15, 88). It is also intriguing that the post stimulus plateau phase is not seen in non-excitable cells following the transmission of $[Ca^{2+}]_c$ signals. Certainly in astrocytes, $[Ca^{2+}]_m$ remains high for a very prolonged period after stimulation (7), suggesting that mitochondrial Ca^{2+} efflux must be very slow and perhaps the activity of the exchanger differs between tissues or cell types.

2.4.4.5. Mitochondrial Ca^{2+} uptake and mitochondrial function

It seems likely that the major functional significance of mitochondrial Ca^{2+} uptake is in the regulation of mitochondrial metabolism. In particular the three major rate limiting enzymes of the citric acid cycle are all upregulated by Ca^{2+} (54). Changes in mitochondrial metabolism in response to changes in $[Ca^{2+}]_c$ were demonstrated in 1992 (20, 73) by measuring changes in mitochondrial NADH and flavoprotein autofluorescence in response to calcium signals in a variety of cell types. These observations showed clearly that (i) mitochondria must be taking up Ca^{2+} during $[Ca^{2+}]_c$ signals, and (ii) that this was sufficient to

activate the TCA cycle. It seems also likely that the transfer of Ca^{2+} from the cytosol to mitochondria during $[Ca^{2+}]_c$ signals represents a major mechanism to couple increased ATP demand with an increase in the supply, as in almost all systems, increases in work are associated with increases in $[Ca^{2+}]_c$. (34) Other observations show that the glutamate/aspartate carrier, responsible for the transport of mitochondrial substrate, is also upregulated by calcium. (43)

Taken together, this all show us what a fundamental role in mitochondrial function Ca^{2+} signals may play. On the other hand under pathological conditions, mitochondrial Ca^{2+} accumulation may also play a key role in determining the outcome, acting as a trigger to pathophysiological events that may dictate the death of the cell. This will be discussed below.

2.3.5. METHODS FOR REDOX STATE DETERMINATION

2.3.5.1. NAD autofluorescence

The term autofluorescence refers to the fluorescence (energy of light) that arises from endogenous compounds intrinsic to the cell. (19) The answer to a question which structures are responsible for such an effect has been clear since 1950s and 60s. (13) It has been showed that the bulk of intrinsic fluorescence in most cells and tissues arises from NADH and flavoproteins of mitochondrial origin. Although many cells also show some non-mitochondrial green/yellow fluorescence whose origin seems less clear. These signals can provide valuable indicators of changes in mitochondrial metabolism, as their properties change with the redox state of the carriers. Briefly the fluorescence of NADH is excited in the UV (peak excitation at about 350 nm) and emits blue fluorescence (with a peak at about 450 nm). (14) The oxidised form, NAD^+, is not fluorescent. An increase in UV-induced blue fluorescence therefore indicates an increase in the ratio of NADH to NAD^+. The pyridine nucleotide pool remains stable in the absolute size but in case of an increase in blue fluorescence has

been shifted to the reduced state in the balance of reduced to oxidized forms. Another pyridine nucleotide NADPH is also fluorescent with very similar spectral properties, but in most cell types, seems to be present at much lower concentrations than NADH. (13)

2.3.5.2. FAD autofluorescence

Flavoproteins which autoflorescence I am measuring in my diploma ferry electrons using a flavin or FAD molecule. Flavoprotein fluorescence is excited in the blue (with a peak at about 450 nm) and fluorescence emission is maximal in the yellow/green, with a peak at about 550 nm. The important thing is that in contrast to NADH, flavoprotein fluorescence decreases when the carrier binds electrons which means is in an oxidized form. And vice versa an increase in flavoprotein autofluorescence reflects a decrease in the ratio of oxidized to reduced form — the inverse of the response of the pyridine nucleotides. The redox state of the pyridine nucleotide and flavoprotein pools reflect the balance between the rate of reduction by substrate processing and the rate of oxidation by mitochondrial respiration. Thus, both upregulation of substrate processing and inhibition of respiration lead the balance towards a reduced state. Conversely, an increase in respiratory rate means an oxidation of the pool. Let me show a nice picture of pyridine nucleotides and flavoproteins autoflorescence here (see Fig. 2.4). For instance if you inhibit the respiration by CN^- or by anoxia, the respiratory chain cannot oxidize the reduced forms which will accumulate to a new steady state. NADH autofluorescence (blue light) increases and flavoprotein autofluorescence (green light) falls. Mitochondrial respiration responds to collapse of mitochondrial membrane potential by an uncoupler with an increase in respiratory rate. This promotes maximal oxidation of NADH to NAD+ and FADH2 to FAD, decreasing the autofluorescence from NADH (blue light) and increasing that from FAD (green light).

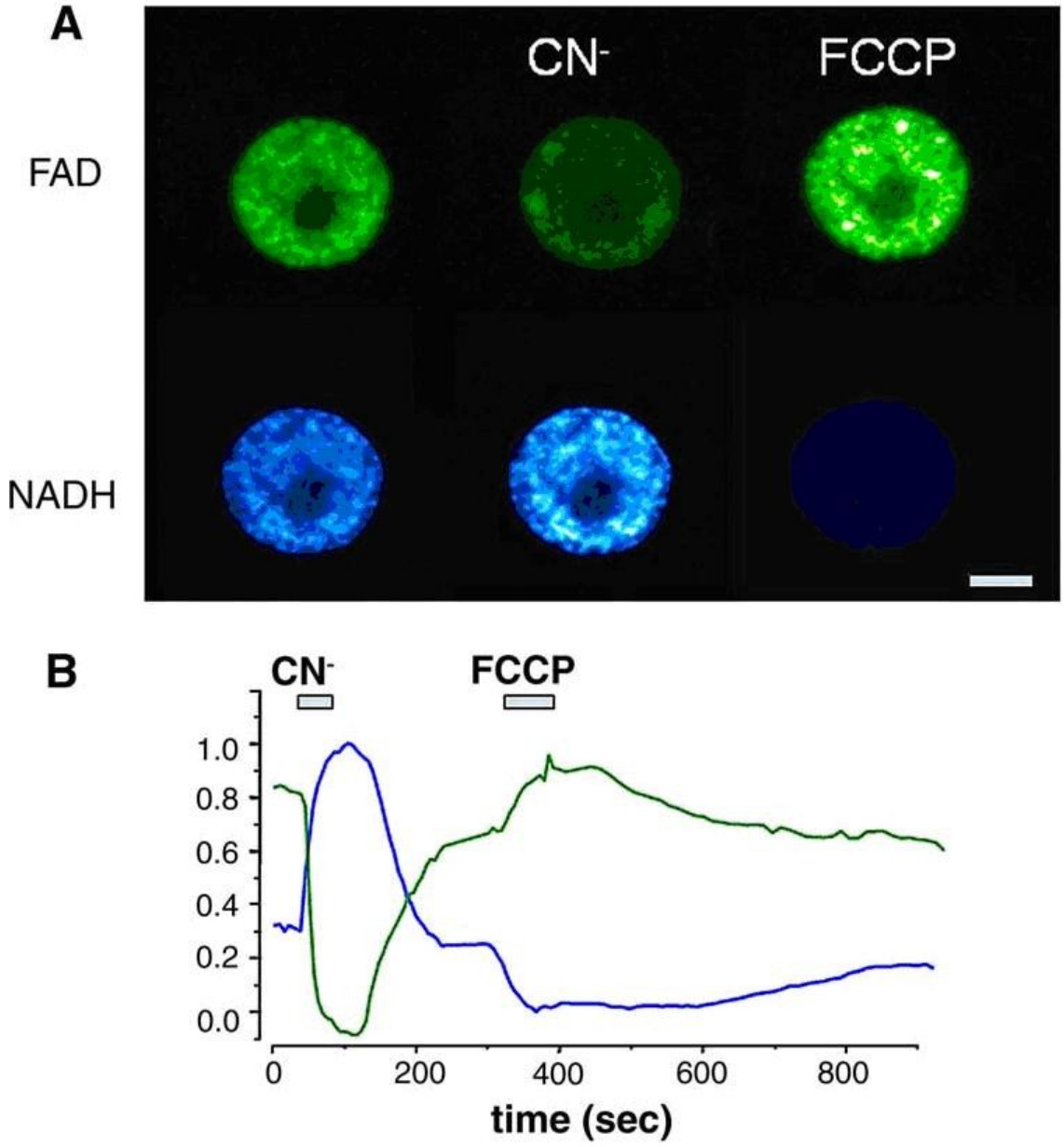

Figure 2.4: *Measurements of redox state.*
(A) Assessing redox state in an adipocyte cell line using cyanide (CN) to promote maximal reduction of flavoproteins and NADH and FCCP to promote maximal oxidation. The confocal system allows sequential switching between excitation at 351 nm (for NAD(P)H measured between 420 and 480 nm) and 458 nm (for flavoproteins, measured at >505 nm). The changing intensities of the two signals are plotted in (B), normalized between the maximally reduced (CN) and maximally oxidized (FCCP) signals.

2.3.5. MITOCHONDRIA AND CELL DEATH

Given the fundamental role of mitochondria as ATP generators and the requirement of cells for ATP to combat the forces of entropy, it seems self-evident that severe damage to mitochondria will cause cell death. Once ATP levels fall, energy dependent processes that include the maintenance of ion gradients, the contraction of muscle, secretion of transmitters, and the maintenance of normal regulation of calcium required for the coordination of calcium signals will inevitably become disordered. Once ionic gradients dissipate, intracellular osmolarity cannot be maintained, and cells will swell and die by a process of necrosis. Not all cells are dependent on mitochondrial oxidative phosphorylation. In the brain, astrocytes seem able to maintain function adequately on glycolytic ATP, while neurons are absolutely dependent on mitochondrial oxidative phosphorylation for normal function, so that we lose consciousness within seconds of oxygen deprivation. That is why one of the key issues is a proper understanding of the main consumers of ATP. This issue does not seem to have been fully resolved. It is often stated that one has 3 minutes to resuscitate a patient with a cardiac arrest before there is significant risk of irreversible brain injury. Presumably that 3 minutes interval (or however long it really is!) is a reflection of the rate of ATP consumption. It is often assumed that the major ATP consumers must be the plasmalemmal ATP-ases—the Ca^{2+}/H^{+} ATPase or the Na^{+}/K^{+} ATPase. However, major changes in intracellular calcium and/or sodium concentrations should not occur until ATP levels have fallen to critical levels. But if it happens and ATP falls under critical level, general features of necrotic cell death including loss of cell membrane integrity, rapid organelle swelling, mitochondrial failure, and energy depletion appear. Cell dies by **necrosis**.

On the contrary cells can die in another way. This process is called programmed cell death, or **apoptosis** (apo "away" + ptosis "fall"). It can be called "cell suicide" in the sense that the cell's own genes play an active role in its demise.

It should be distinguished from necrosis ("cell murder"), in which healthy cells are destroyed by external processes such as inflammation.

Apoptosis is a very common process during development and in adulthood. In the central nervous system, large numbers of neurons are produced and then die during the remodeling that occurs during development and synapse formation. In the immune system, apoptosis gets rid of inappropriate clones of immunocytes. Apoptosis is also an important factor in processes such as removal of the webs between the fingers in fetal life and regression of duct systems in the course of sexual development in the fetus In adults, it participates in the cyclic breakdown of the endometrium that leads to menstruation. In epithelia, cells that lose their connections to the basal lamina and neighboring cells undergo apoptosis. This is responsible for the death of the enterocytes sloughed off the tips of intestinal villi. Abnormal apoptosis probably occurs in autoimmune disease, neurodegenerative diseases, and cancer.

2.4. NEURODEGENERATIVE DISEASE AND MITOCHONDRIA

The neurodegenerative diseases represent a significant cause of concern in the health professions today. These diseases are unfortunately debilitating including Alzheimer's disease, Parkinson's disease, Motor neuron disease (amyotrophic lateral sclerosis, or ALS, also known as Lou Gehrig's disease in the USA), multiple sclerosis (MS), injury to the CNS through, chronic low grade hypoxia and the rarer but crippling Huntington's disease, Wilson's disease and Freidreich's Ataxia. A number of inherited disorders of the mitochondrial genome known as mitochondrial encephalomyopathies also cause disorders of the CNS. And there are, of course, more such diseases. What they all have in common is that the fundamental pathophysiological mechanisms remain unclear, but in all, mitochondrial function has been impaired at some level of the pathogenic process. Thus contemporary neuroscience is trying to

understand the basic pathways that lead to the development of mitochondrial diseases.

2.4.1. MOTOR NEURON DISEASE

Motor neuron disease or amyotrophic lateral sclerosis (ALS) is an appalling and debilitating disease which causes the selective degeneration of motoneurons, weakness and death after a few years. We know remarkably little about the cause of motoneuron degeneration, and understand even less of the mechanisms that make that degeneration selective for one population of cells. There is quiet a widespread view that the primary mechanism of motoneuron injury involves calcium overload and mitochondrial damage.

2.4.2. ALZHEIMER'S DISEASE

Alzheimer's disease is the most common form of dementia, and it is by definition characterised by the accumulation in the brain of extracellular neuritic plaques, together with the presence of intraneuronal neurofibrillary tangles (NFT) and progressive neurodegeneration. The plaques are mainly composed of amyloid-ß (Aß), a peptide, forming large insoluble fibrillary aggregates, and are surrounded by dystrophic neurites and activated glial cells. While the role of this peptide in the development of the pathology is not yet clear, excessive accumulation of Aß—either due to excess production or reduced clearance—appears to be sufficient to cause the disease. (58) Thus, patients with Down's Syndrome, who have an extra copy of the chromosome carrying the gene for the Aß precursor protein (APP), develop plaques and dementia at an early age. Indeed, all the known mutations associated with familial Alzheimer's disease are in the genes for APP or for the presenilins, enzymes involved in the processing of APP—all of which result in Aß overproduction.

2.4.3. HUNTINGTON'S DISEASE

Huntington's disease (HD) is caused by an expansion of exonic CAG triplet repeats in the gene encoding the protein known as Huntingtin (Htt). It has been (66) found that mitochondria isolated from lymphoblasts of patients with HD had a lower membrane potential than mitochondria from control subjects. They also found that upon calcium addition, the mitochondria depolarized in response to smaller calcium loads than mitochondria from controls. They found a similar response in mitochondria extracted from the brains of transgenic mice which express the full-length mutant protein, huntingtin. Interestingly, this defect preceded the onset of pathological or behavioral abnormalities by months. The mutant huntingtin could be seen on neuronal mitochondrial membranes using electron microscopy with imunolabelling. Further and remarkably, incubation of normal mitochondria with a fusion protein containing an abnormally long polyglutamine repeat reproduced the mitochondrial calcium defect seen in human patients and transgenic animals. The authors suggested that, mitochondrial calcium abnormalities occur early in HD pathogenesis and may be a direct effect of mutant huntingtin on the organelle. (10)

2.4.4. PARKINSON'S DISEASE

There is a considerable body of evidence that links abnormalities of mitochondrial Complex I with the selective degeneration of nigro-striatal neurons in Parkinson's disease. (42) Complex I deficiency has also been widely reported in the substantia nigra of patients with sporadic PD. (69, 56, 81) It has even been suggested on epidemiological grounds that at least in some patients, the disease may reflect environmental exposure to the insecticide rotenone, the classical inhibitor of complex I. What does seem extraordinary is that the systemic administration of low doses of rotenone to rats seems to cause a PD like syndrome which includes the selective degeneration nigro-striatal neurons and the appearance of synuclein rich inclusion bodies which are a feature of the

disease. (83) The specific site of action of rotenone seems unambiguously defined as mitochondrial complex I—the drug is relatively selective, and the same group remarkably also managed to transfect into cells a yeast subunit of complex I which lacks the rotenone binding site, and cells became resistant to rotenone (84)—although of course this tells us little about the action of the drug in the whole animal. It seems that cell injury is not 'simply' a function of metabolic insufficiency, as similar degrees of ATP depletion induced by other poisons (inhibition of glycolysis with 2-deoxyglucose) failed to cause the same injury. Rather, cells could be protected with antioxidants, suggesting that the primary mechanism of injury is through oxidative stress. Complex I is particularly vulnerable to modification by oxidative stress, and in turn is a potential generator of reactive oxygen species – very reactive molecules that can damage membranes. What seems so extraordinary to me is that given systemic administration of a poison which targets complex I in all tissues, the poison primarily attacks striatal neurons. Why are these neurons so selectively vulnerable? What happens in other parts of the brain?

The greatest puzzle in almost all of the neurodegenerative diseases is the way in which a widespread pathology can cause selective degeneration in a subset of neurons—rotenone toxicity which only affects striatal neurons, the polyglutamine repeats that cause degeneration of basal ganglionic neurons and so on. In all of these cases, we seem to see some interplay between oxidative stress and mitochondrial dysfunction, but in no case do we have a really satisfactory answer to explain the selectivity of the disease phenotype.

3. AIMS AND HYPOTHESIS

3.1. AIMS

The aim of this study was to determine the influence of temperature and stimulus intensity on FAD transience in rat hippocampal slices in vitro.

3.2. HYPOTHESIS

I. We hypothesized that FAD fluorescence signals would rise depending on increased temperature. We expected this phenomenon mainly because of the fact that increased temperature kept more molecules in their excited states so they were more likely to become fluorescent.

II. We expected that FAD fluorescence would rise during stimulation as a result of increased metabolic demands during stimulation.

4. METHODS

4.1. CHARACTERIZATION OF THE GROUP OF ANIMALS

Experiments were performed on slices prepared from adult male Wistar albino rats (100-180g). Rats were housed in a controlled environment (temperature 22 ± 1°C, humidity 50-60%, lights on 06:00-18:00 h) with free access to food and water. Experiments were approved by the Animal Care and Use Committee of the Institute of Physiology of the Academy of Sciences of the Czech Republic. Animal care and experimental procedures were conducted in accordance with the guidelines of the European Community Council directives 86/609/EEC.

4.2. SLICE PREPARATION AND MAINTENANCE

For the purpose of this study we have used live brain tissue slices. Rats were deeply anaesthetized with ether and decapitated. Brain was rapidly removed from the scull, cut in oxygenated (95%) and cooled (-0,5°C) artificial cerebrospinal fluid (ACSF) using vibratome in coronal slices of 400μm of thickness. The slices contained both the somatosensory cortex and the hippocampus and were transferred immediately after the preparation to a holding chamber. After 120 minutes recovery they were submerged into recording chamber through which oxygenated ACSF was perfused (2 ml/min) using a peristaltic pump. The composition of this perfusion solution was (in mM): 126 NaCl; 26 $NaHCO_3$; 1.8 KCl; 1.25 KH_2PO_4; 1.3 $MgSO_4$; 2.4 $CaCl_2$; 10 glucose.

4.3. ELECTROPHYSIOLOGICAL SYNAPTIC ACTIVATION

Synaptic activation of the tissue was being made with bipolar stimulating electrode placed in hillus of the dentate gyrus of hippocampus (Mossy fibers). For field potentials recording extracellular glass microelectrodes (8-10 M Ω) filled with 1 M NaCl was used and placed in pyramidal layer of CA3 region (see Fig. 4.1). 10 minutes after the replacement of the slice into the recording chamber, single shock stimulation characteristic were applied and field responses were recorded. When stable evoked field potentials were detected, the stimulus threshold (T) was determined. After that a series of 10s stimulus train with different intensities (2T, 3T, 4T) were delivered for the stimulation and parallel detection of FAD fluorescence were performed. Each slice was firstly maintained at 26°C and activated with rising intensities: 2T, 3T, 4T, than temperature was switched to 36°C and again the slice was activated with the same rising intensities of 2T, 3T and 4T. The recovery period between each activation was 5 minutes.

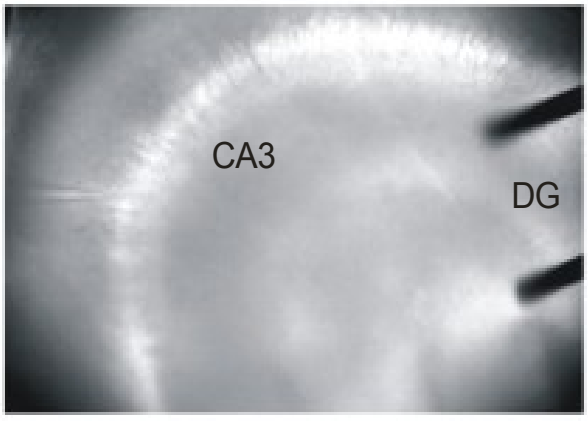

Figure 4.1: *Fluorescence microscope image*(20/0.5) (Olympus BX51WI) on the right side, there is stimulating electrode placed in DG (dentate gyrus) of hippocampus, on the left, we can see registrating electrode in the pyramidal layer of CA3 region of hippocampus.

4.4. FAD AUTOFLUORESCENCE SIGNALS DETECTION

Cooled 12-bit CCD-camera (RETIGA2000R) was used for detection of the flavoprotein signals. Images are analyzed using anatomically based regions of interest (ROI), generating a series of 12-bit (averaged across multiple pixels) intensity numbers for plotting, as a function of time. The 12-bit pixel values are linear and proportional to the absolute lightlevel. Difference images were also calculated for each series on a pixel by pixel basis, using a control image as a baseline for each further image in the series:

$$\Delta I / I = (\mathrm{Image}_i \;\; \mathrm{Image}_{control}) / \mathrm{Image}_{control}$$

4.5. STATISTICS

The statistic data were evalutated using the software Sigma Plot version 10.0, Systat Software Inc., (see Fig. 5.1 and Fig. 5.5) and Sigma Stat version 3.5, Systat software Inc., using descriptive statistics and paired t-test (see Att. 2 -4). The Paired t-test examines the changes which occur before and after a single experimental intervention on the same individuals to determine whether or not the treatment had a significant effect. Examining the changes rather than the values observed before and after the intervention removes the differences due to individual responses, producing a more sensitive, or powerful, test.

5. RESULTS

We have analyzed the total amount of 6 rad hippocampal slices. In four slices we evaluated one region of interest (ROI), at the highest FAD autofluorescence signal during 2T stimulus intensity at the temperature of 26°C. The ROI was later investigated at T3 and 4T stimulus intensity at 26°C and 2T, 3T, 4T stimulus intensity at 36°C. We determined ROIs with the highest FAD autoflorescence signal in each slice, disregarding the FAD signals from different layers of the CA of hippocampus.

To obtain more complex data, in the last two slices, we focused on 9 different ROIs in each slice trying to show 3 FAD autoflorescence signals from *stratum radiale*, 3 from *stratum pyramidale* and 3 from *stratum oriens* (see Att. 5). We choose the ROIs so, that they formed 3 columns – each column containing 1 ROI from different layer. The columns included all layers at different distances from the stimulating electrode. So that we could evaluate the FAD signal in the certain distance from the electrode and compare the different layers.

Surprisingly our first hypothesis has not been confirmed. On the contrary, the data showed that in all 6 slices FAD autofluorescence signals were significantly decreased at higher temperature level (see Fig. 5.1). We further revealed FAD autofluorescence and different stimulus intensity dependency.

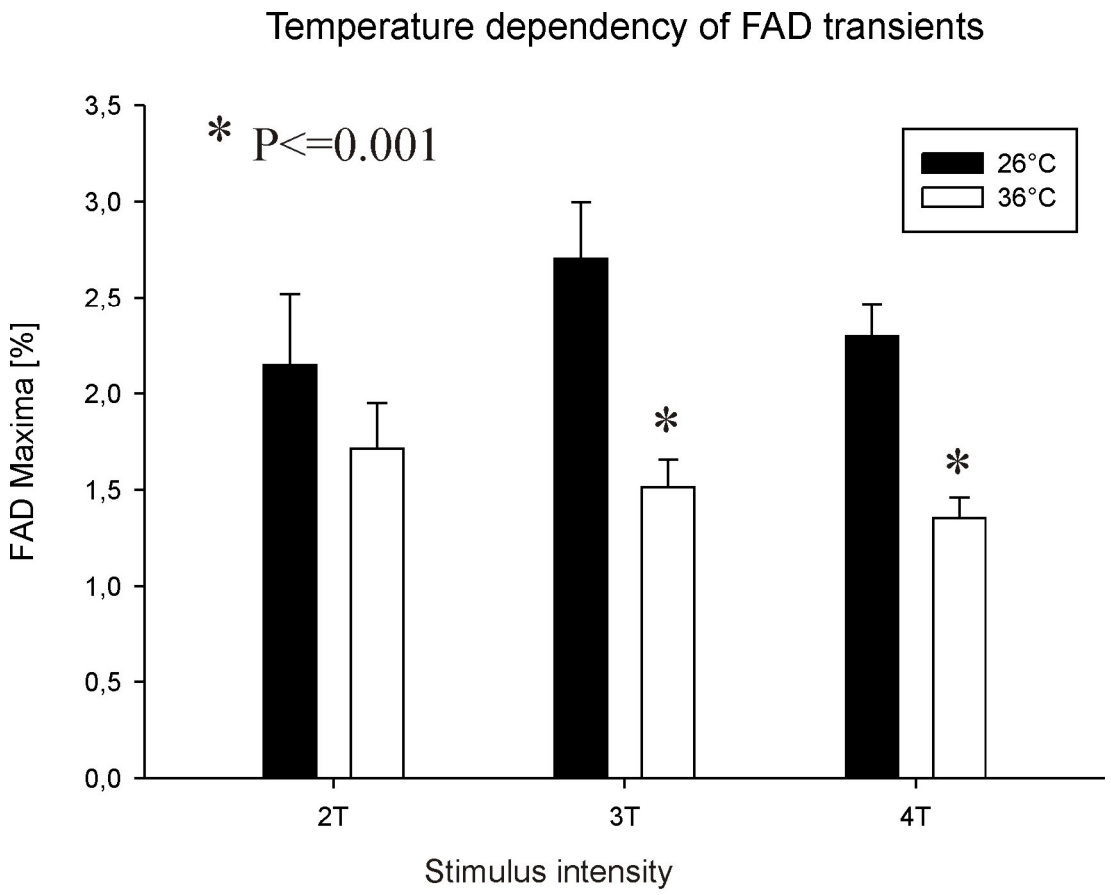

Figure 5.1: Temperature dependency of FAD transients signals at different stimulus intensities; FAD signal maximal values.

5.1. FAD FLUORESCENCE SIGNALS AND TEMPERATURE

Our data showed that FAD autofluorescence signals were decreased at higher temperature. There has been significant difference decrease in all 6 slices in flavoprotein signals at 3T and 4T stimulus intensity between the lower (26°C) and higher (36°C) temperature level. We further investigated this phenomenon in more detail. The temperature dependency was compared in two slices using 9 ROIs in each (as described above). The data confirmed our previous results. FAD autofluorescence signals show smaller light intensity in different layers of CA3 under the same conditions at 36°C compared 26°C (see Fig. 5.2).

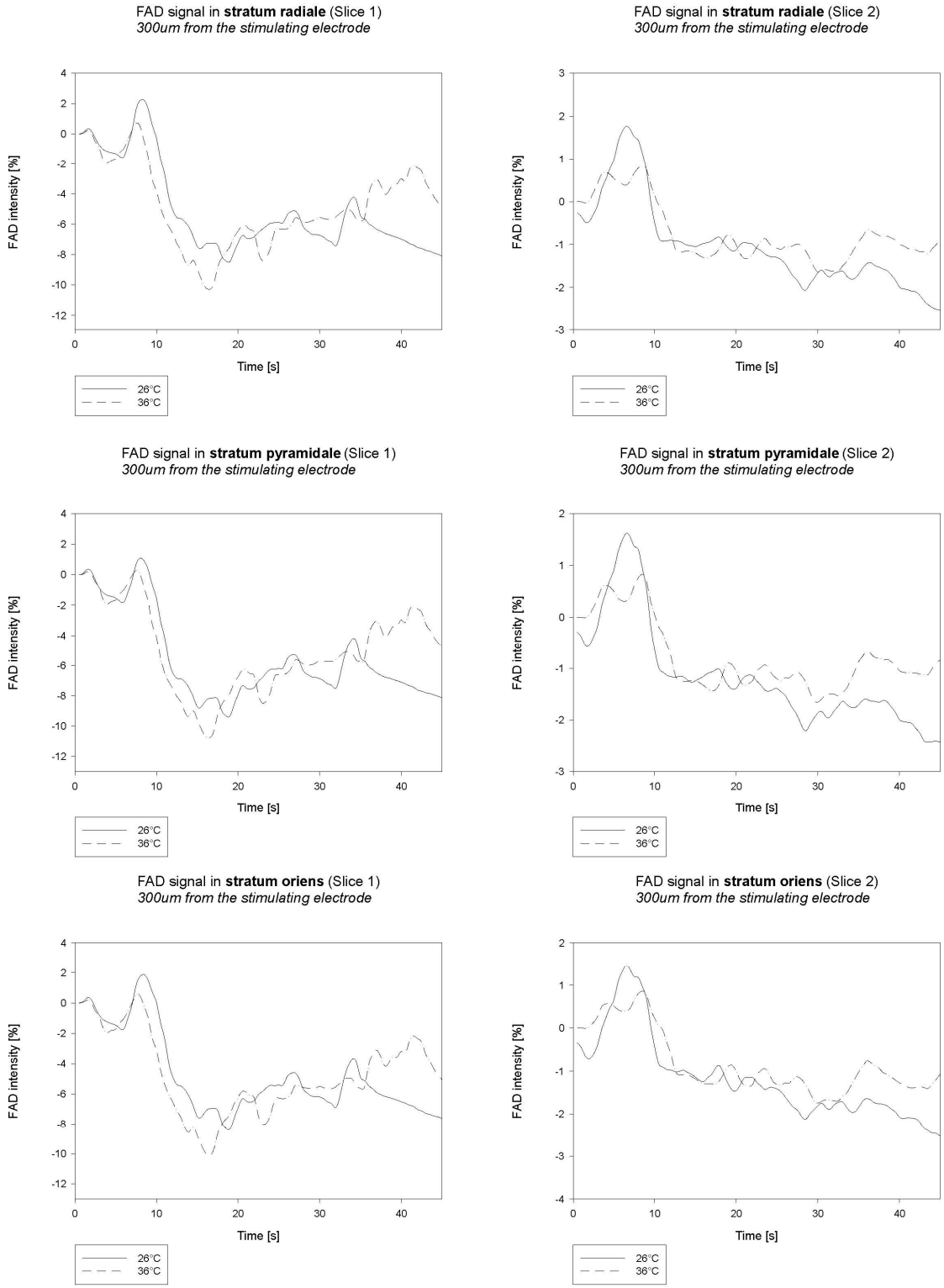

Figure 5.2: FAD signals in stratum radiale, stratum pyramidale and stratum oriens at lower (26°C) and higher (36°C) temperature in two different slices. ROIs were placed 300um from the stimulating electrode.

5.2. FAD FLUORESCENCE SIGNALS AS A FUNCTION OF INCREASING STIMULUS INTENSITY

In terms of different stimulus intensity, our data showed that flavoprotein autofluorescence signals increased under the same conditions upwardly in ROIs placed more distantly from the stimulating electrode in each layer – *stratum radiale*, *stratum pyramidale* and *stratum oriens*. The more distantly the ROI was placed in each layer from the stimulating electrode, the higher FAD autofluorescence signals have been detected (see Fig. 5.3).

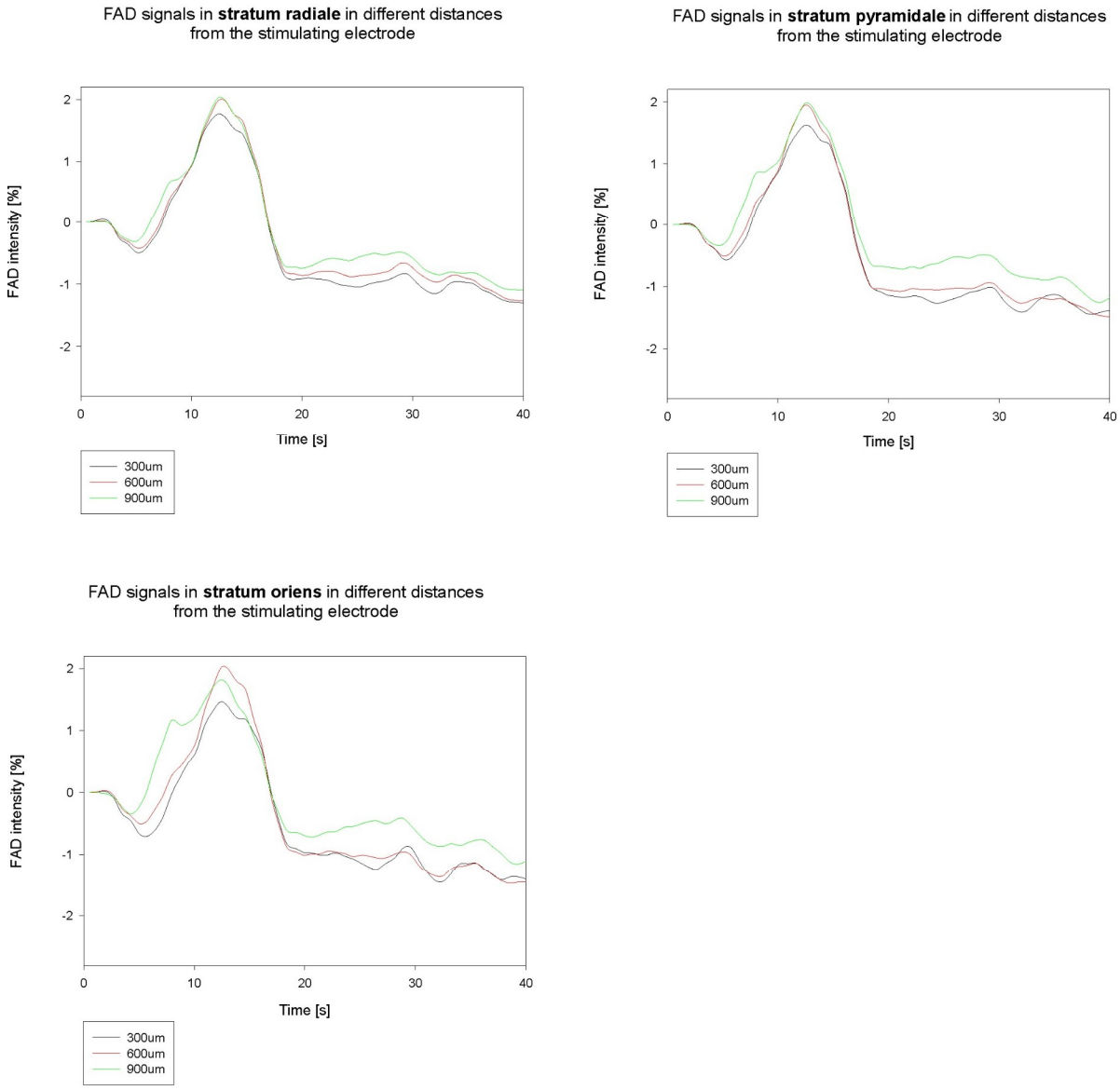

Figure 5.3: FAD signals in stratum radiale, stratum pyramidale and stratum oriens in distances 300um, 600um and 900um from the stimulating electrode in one slice. Each paragraph shows FAD signals from the same layer in different distances in one slice.

When we compared the ROIs from different layers at the same distance from the stimulating electrode (within one column as described above), the flavoprotein autofluorescence signals has not differed significantly (see Fig. 5.4).

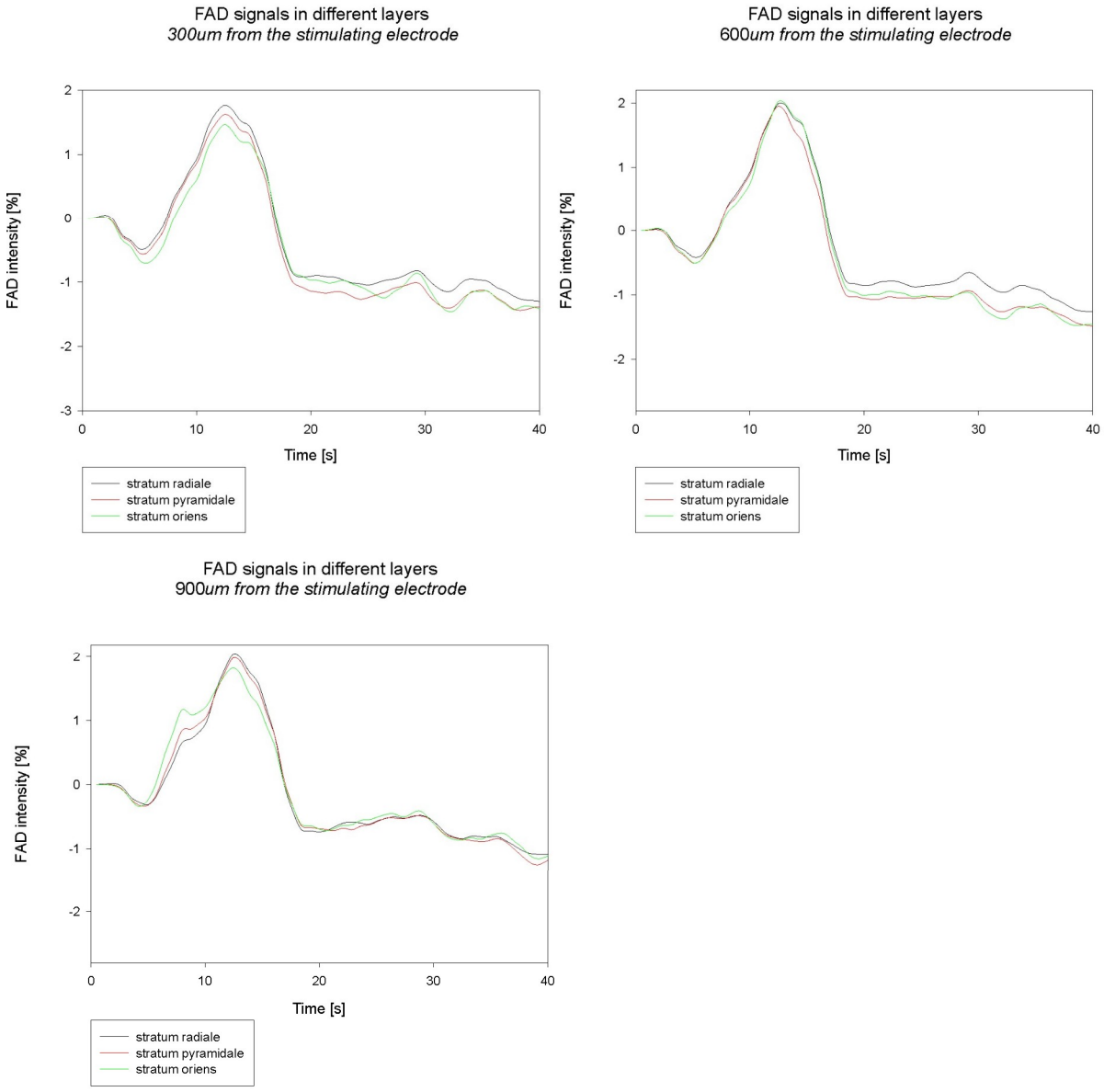

Figure 5.4: FAD signals in stratum radiale, stratum pyramidale and stratum oriens in distances 300um, 600um and 900um from the stimulating electrode. Each paragraph shows FAD signals in the same distance in different layers in one slice.

There had also been no significant difference in the time (time latency) in which maximal FAD autofluorescence signals were achieved after the start of series of 10s stimulus train (see Fig. 5.5).

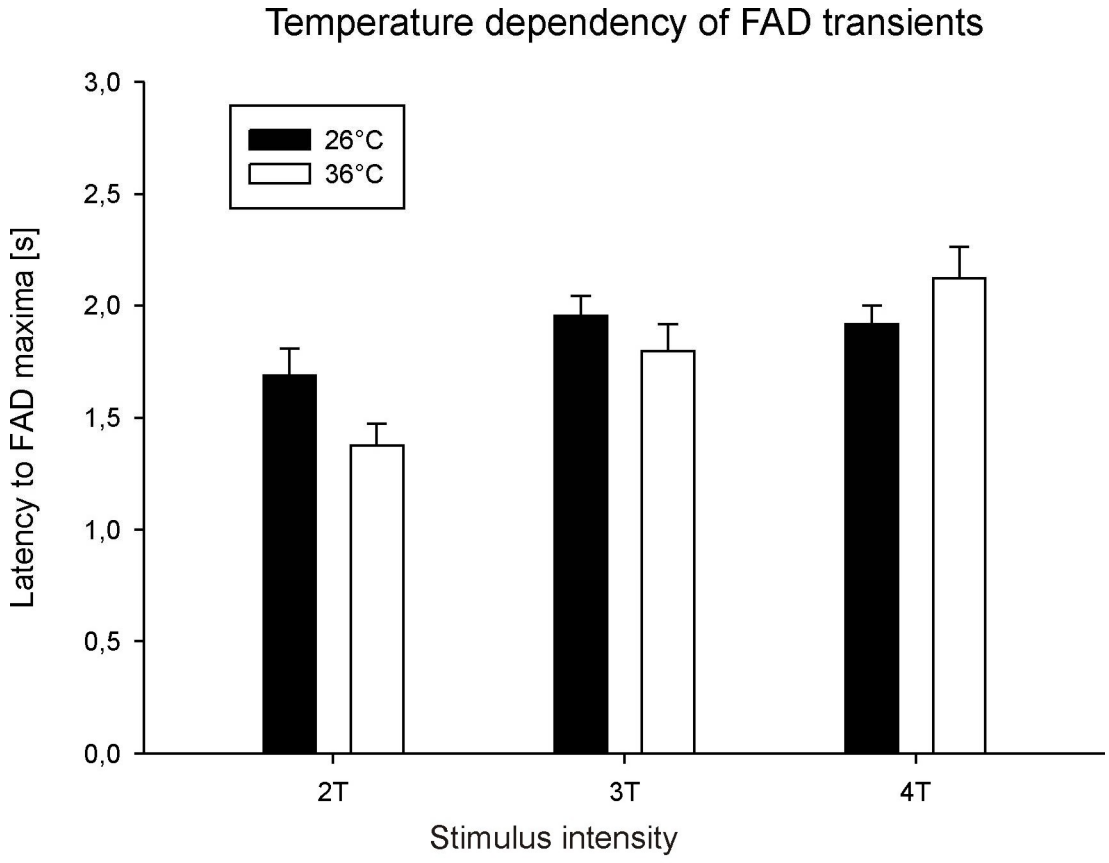

Figure 5.5: Temperature dependency of FAD transients signals at different stimulus intensities; time latency to FAD maximal values.

6. DISCUSSION

6.1. DISCUSSION - THE METHODS

For the purpose of our study rat hippocampal slices were used. The relatively well established method is simple and offers the possibility to see right onto the tissue with all the cells that are present. (2)

The fact that we were using so called submerged recording chamber where the slice was surrounded by ACSF reminded more in vivo conditions. In vivo there is also not gaseous atmosphere present like in the interface type of the chamber but the cells are in contact and surrended by liquid tissue. The source of some kind of the noise that could influence the detection of the signal is permanent flow of the ACSF (4ml/min) that has to be present around the slice.

There are unfortunately still some crucial differences compared with the real organism such as the slower washout of the ions from the extracellular space (15) and especially what is in our interest, the difference in oxygen availability that could cause apparent discrepances in the assessment of the mitochondrial function and its reaction to the stimulation. (92)

In the non-vascular tissue, the oxygen is further delivered into the tissue only through the diffusion and does not react on the energy demand via increase in blood flow which would normally occurred in vivo after the stimulation.

6.2. DISCUSSION - THE RESULTS

Recently, there is an increased interest in the research concerning restriction in the mitochondrial function and its role in the pathophysiology of various diseases such as Parkinson's, Alzheimer's or various motor neuron diseases. The aim of this study was to elucidate the role of mitochondrial FAD autofluorescence for the detection of mitochondrial activity in the slices of the

nervous tissue during the increasing stimulus intensity which is followed by higher metabolic demand and at various temperatures to get to know more about mitochondrial function in these certain conditions.

Our results show indeed that we can use the flavoprotein autofluorescence signal for the assessment of the mitochondrial metabolic functions. FAD is important marker because of its role as an intermediate providing reducing equivalents to the respiratory chain which consist of series of enzyme systems. (19) In particular, the stimulation (20Hz/10s) of the mossy fibers of Dentate Gyrus of the hippocampus resulted in increase of FAD signals in the CA3 region of the hippocampus as the metabolic demand augmented. The electrical stimulation provoked as noted above the energy demand. The signals of mitochondrial origin react on this demand. FAD is oxidized in the respiratory transport chain, followed by regeneration in the trichloroacetic acid cycle (Crebs cycle) which further decrease the FAD signal (8) and this also corresponds with our findings.

The other data that we could evaluate were the distance from the stimulation site. The shorter was the distance between the stimulating electrode and the analyzed area (ROI), the more pronounced was the FAD fluorescence signal which also corresponds to the previous notion that the FAD signal is of mitochondrial origin and comes into line with our hypothesis that the signal is coupled with the electrical stimulation.

The FAD signal we detected further did not reveal the differences in the various tissue layers in terms of its spread and not even in the intensity of the signal. According to our presumption there could be some variances observed since there is a difference in metabolic processes that are proceeding in subsarcolemal and interfibrilar mitochondria, in other terms the mitochondria observed in the proximity of the synapses could modulate the FAD signal differently than mitochondria of the neuronal body. (19) Or there is also the

possibility that FAD signal could not be strong enough to distinguish among the layers.

The most important finding was the decrease of FAD signal in the conditions with the higher temperature which did not fit with our previous presumption. We hypothesized that FAD fluorescence signals would rise depending on increased temperature that should keep more molecules in their excited states so they would be more likely to become fluorescent but this was not the case. We had to therefore think of the other causes that would overlap this effect of the temperature. In the literature we found that the FAD signal can be decreased in the hypoxic conditions in vivo (85). The diffusion of oxygen was probably increased with the higher temperature, which was followed by the remarkably increased metabolism demand, and this was even more than would cover the increased oxygen diffusion. Another fact taken into the account is the effect of higher temperature on the blockage of mitochondrial respiration. There were observed for example different temperature dependent levels of cytochrome c. (35)

Therefore further experiments should be done to fully elucidate the role of the temperature on the autofluorescence and FAD signal to make broader conclusions. This diploma thesis is a pivotal study in this field.

7. CONCLUSIONS

Our observations have not supported the hypothesis that FAD fluorescence signals would be risen with increased temperature. On the contrary the opposite effect was observed. Our data showed that increased temperature significantly decreased FAD autofluorescence signals. Focusing on this phenomenon in more detail our data strongly suggest that FAD autofluorescence signals show smaller light intensity in different layers of CA3 at the higher temperature (36°C) compared to the lower temperature (26°C).

Our second hypothesis has been confirmed. Our data showed that under defined conditions FAD fluorescence signals have risen during stimulation. We concluded that fact as a result of increased metabolic demands during stimulation.

8. ABBREVIATIONS

Aß - amyloid-ß

ACSF – Artificial Cerebrospinal Fluid

ALS - Amyotrophic Lateral Sclerosis

APP - Amyloid-ß Precursor Protein

ATP - Adenosine triphosphate

Ca – Calcium

CA1-3 - Region 1-3 of the Cornu Ammonis

CNS - Central Nervous System

CO_2 – Carbonyle Dioxyde

CoA – Coenzyme A

DNA - Deoxyribonucleic acid

DG - Dentate Gyrus

EC - Entorhinal Cortex

FAD - Flavinadenindinucleotide

HC – Hippocampus

HD - Huntington's disease

Htt - Huntingtin

K - Potassium

ms – Millisecond

MS – Multiple Sclerosis

mV - Millivolt

Na - Natrium

NAD.- Nicotinamidadenindinucleotide

NADP - Nicotinamidadenindinucleotidphosphate

NFT - Neurofibrillary Tangles

ROI – Region of Interest

TCA - Tricarboxylic acid

VDAC - Voltage-dependent anion channel

9. REFERENCES

1. AMARAL, D. G., WITTER, M. P. Hippocampal formation. In: *The Rat Nervous System*, 2nd ed., Sydney: Academic Press Inc. 1995, Chapter 21, pp. 443-493.

2. ANDERSEN, P., BLISS, T. V., SKREDE, K. K. Lamellar organization of hippocampal excitatory pathways. *Exp. Brain Res.*, 1971, vol. 13, pp 222-238.

3. ANDERSEN, P. Brain slices – a neurobiological tool of increasing usefulness. *Acta Physiologica Scandinavica,* 1981;113(3):355-62.

4. BABCOCK, D. F.,HERRINGTON, J., GOODWIN, P. C., PARK, Y. B., HILLE, B. Mitochondrial participation in the intracellular Ca^{2+} network. *J. Cell Biol,* 1997, 136 (4), 833–844.

5. BAUMANN, N., PHAM-DINH, D. Biology of oligodendrocyte and myelin in the mammalian central nervous system. *Physiological Reviews*, April 2001, vol. 81, no. 2, pp. 871-927.

6. BERNARDI, P., AYYONE, G. F. A membrane potential-modulated pathway for Ca^{2+} efflux in rat liver mitochondria. *FEBS Lett.*, 1982, 139, 13–16.

7. BOITIER, E., REA, R., DUCHEN, M. R. Mitochondria exert a negative feedback on the propagation of intracellular Ca^{2+} waves in rat cortical astrocytes. *J. Cell Biol.*, 1999, 145 (4), 795–808.

8. BRENNAN, A. M., CONNOR, J. A., SHUTTLRWORTH, C. W. NAD(P)H fluorescence transients after synaptic activity in brain slices: predominant role of mitochondrial function. *Journal of Cerebral Blood Flow and Metabolism,* November 2006, vol. 26, no. 11, pp. 1389-1406.

9. BRUMM, D. *Focal Cooling: An intrinsic optical imaging study of the effect of cooling a 4-aminopyridine induced focal seizure* Saint Louis: 2007, pp. 54. A Thesis - Presented to the Faculty of the Graduate School of the University of Missouri. Supervisor Dr. Bahar.

10. BRUSTOVETSKY, N., BRUSTOVETSKY, T., PURL, K. J., CAPANO, M., CROMPTON, M., DUBINSKY, J. M. Increased susceptibility of striatal mitochondria to calcium-induced permeability transition. *J. Neurosci.*, 2003, 23 (12), 4858–4867.

11. CAFFERTY, W.B., STRITTMATTER, S.M. The Nogo-Nogo receptor pathway limits a spectrum of adult CNS axonal growth. *The Journal of Neuroscience*, November 2006, vol. 26, no. 47, pp. 12242-12250.

12. CAPAGNONI, A.T. Molecular Biology of Myelination, In: *Neuroglia*, 2nd edition, New York: Oxford University Press 2004, Chapter 19, pp. 253-263.

13. CHANCE, B., BALTSCHEFFSKY, H. Respiratory enzymes in oxidative phosphorylation. VII. Binding of intramitochondrial reduced pyridine nucleotide. *J. Biol. Chem.*, 1958, 233 (3), 736–739.

14. CHANCE, B., SCHOENER, B., OSHINO, R., ITSHAK, F., NAKASE, Y. Oxidation–reduction ratio studies of mitochondria in freeze-trapped samples. NADH and flavoprotein fluorescence signals. *J. Biol. Chem.*, 1979, 254, 4764–4771.

15. CRONING, M. D., HADDAD, G. G. Comparison of brain slice chamber designs for investigations of oxygen deprivation in vitro. *Journal of neuroscience methods,* 1998 Jun 1;81(1-2):103-11.

16. DAVID, G., BARRETT, J. N., BARRETT, E. F. Evidence that mitochondria buffer physiological Ca^{2+} loads in lizard motor nerve terminals. J. Physiol., 1998, 509, 59–65.

17. DENG, Y., MARKO, M., BUTTLE, K. F., LEITH, A., MIECZKOWSKI, M., MANNELLA, C. A., Cubic membrane structure in amoeba (Chaos carolinensis) mitochondria determined by electron microscopictomography. *J. Struct. Biol.*, 1999, 127, 231–239.

17. DIRNAGL, U., IADECOLA, C., MOSKOWITZ, M. A. Pathobiology of ischemic stroke: an integrated view. *Trends in Neurosciences*, September 1999, vol. 22, no. 9, pp. 391-397.

18. DOBKIN, B. H. Behavioral, Temporal, and Spatial Targets for Cellular Transplants as Adjuncts to Rehabilitation for Stroke. *Stroke.* February 2007, vol. 38, no. 2, pp. 832-839.

19. DUCHEN, M. R. Mitochondria in health and disease: perspectives on a new mitochondrial biology. *Molecular Aspects of Medicine*, 2004, vol. 25, pp. 365-451.

20. DUCHEN, M.R., LEYSSENS, A., CROMPTON, M. Transient mitochondrial depolarizations reflect focal sarcoplasmic reticular calcium release in single rat cardiomyocytes. J. Cell Biol., 1998, vol. 142, no. 4, pp. 975–988.

21. ENRIGHT, L. E., ZHANG, S., MURPHY, T. H. Fine mapping of the spatial relationship between acute ischemia and dendritic structure indicates selective vulnerability of layer V neuron dendritic tufts within single neurons in vivo. *Journal of Cerebral Blood Flow & Metabolism,* June 2007, vol. 27, no. 6, pp. 1185-1200.

22. FEYDY A., et al. Longitudinal study of motor recovery after stroke: recruitment and focusing of brain activation. *Stroke*, June 2002, vol. 33, no. 6, pp. 1610-1617.

23. FOURNIER, A. E., et al. Truncated soluble Nogo receptor binds Nogo-66 and blocks inhibition of axon growth by myelin. *The Journal of Neuroscience,* October 2002, vol. 22, no. 20, pp. 8876-8883.

24. FOWLER, J.H. Intracerebral injection of AMPA causes axonal damage in vivo. *Brain Research*, November 2003, vol. 991, no. 1-2, pp. 104-112.

25. FRANK, J., WAGENKNECHT, T., McEWEN, B. F., MAKRO, M., HSIEH, C. E., MANNELLA, C. A. Three- dimensional imaging of biological complexity. *J. Struct. Biol.*, 2002, 138, 85–91.

26. FREY, T. G., MANNELLA, C. A. The internal structure of mitochondria. *Trends Biochem. Sci*., 2000, 25, pp. 319–324.

27. GANONG W. F. In: *Review of Medical Physiology*, 22nd ed., USA: McGraw Hill Companies, Inc., 2005, Chapters 2-4, pp. 51-128.

28. GINCEL, D., ZAID, H., SHOHAN-BARMATS, V. Calcium binding and translocation by the voltage-dependent anion channel: a possible regulatory mechanism in mitochondrial function. *Biochem J*., 2001, 358, pp. 147–155.

29. GÓMEZ-DI CESARE, C. M., et al. Axonal remodeling during postnatal maturation of CA3 hippocampal pyramidal neurons. *The Journal of Comparative Neurology*, July 1997, vol. 384, no. 2, pp. 165-180.

30. GOLDSTEIN L. B., et al. A Guideline from the American Heart Association/American Stroke Association. *Stroke*, June 2006, vol. 37, no. 6, pp. 1583-1633.

31. *Gross Anatomy* [online]. © 2006 [cit. 2008-02-05]. URL: <http://www.blackwellpublishing.com/patestas/chapters/6.pdf>

32. GUAN, J., et al. Selective neuroprotective effects with insulin-like growth factor-1 (IGF-1) in phenotypic striatal neurons following ischemic brain injury in fetal sheep. *Neuroscience*, December 1999, vol. 95, no. 3, pp. 831-839.

33. HAJNOCZKY, G., HAGER, R., THOMAS, A. P. Mitochondria suppress local feedback activation of inositol 1,4,5-trisphosphate receptors by Ca^{2+}. *Biol. Chem*., 1999, vol. 274, no. 20, pp. 14157–14162.

34. HORIKAWA, Y., GOEL, A., SOMLYO, A. P., SOMLYO, A. V. Mitochondrial calcium in relaxed and tetanized myocardium. *Biophys. J*., 1998, 74, pp. 1579–1590.

35. HSIEH, C. E., MARKO, M., FRANK, J., MANNELLA, C. A. Electron tomographic analysis of frozen-hydrated tissue sections. *J. Struct. Biol*., 2002, 138, pp. 63–73.

37. KANN, O., SCHUCHMANN, S., BUCHHEIM, K., HEINEMANN, U. Coupling of neuronal activity and mitochondrial metabolism as revealed by NAD(P)H fluorescence signals in organotypic hippocampal slice cultures of the rat. *Neuroscience*, 2003, vol. 119, pp. 87-100.

38. KOISTINAHO, M., KOISTINAHO, J. Interactions between Alzheimer's disease and cerebral ischemia - focus on inflammation. *Brain research. Brain research reviews*, April 2005, vol. 48, no. 2, pp. 240-250.

39. KOIVISTO, A. Genetic components of late-onset Alzheimer's disease with special emphasis on ApoE, IL-6, CYP46, SERPINA3 and PPARγ. Series of reports, No. 81, Department of Neurology, University of Kuopio 2006, p. 112.

40. KONOPKOVÁ, R. Changes in Hippocampal Volume after Application of NMDA. Praha, 2005. *Diplomová práce* na Fakultě Tělesné Výchovy a Sportu Univerzity Karlovy, katedře fyzioterapie. Vedoucí diplomové práce MUDr. Jakub Otáhal, Ph.D.

41. KLUSMAN, I., SCHWAB, M. E. Axonal Regeneration in the Central Nervous System of Mammals, In: *Neuroglia*, 2nd edition, New York: Oxford University Press 2004, Chapter 37, p. 467-476.

42. LANGSTON, J. W., BALLARD Jr., P. A. Parkinson's disease in a chemist working with 1-methyl-4-phenyl-1,2,5,6-tetrahydropyridine. *N. Engl. J. Med.*, 1983, vol. 309, no. 5, p. 310.

43. LAROSA, F. M., PINTON, P., PALMIERI, L., FIERMONTE, G., RIZZUTO, R., PALMIERI, F. Recombinant expression of the Ca^{2+} -sensitive aspartate/glutamate carrier increases mitochondrial ATP production in agonist-stimulated Chinese hamster ovary cells. *J. Biol. Chem.*, 2003, vol. 278, no. 40, pp. 38686–38692.

44. LEKKER, R. R., et al. Novel Therapies for Acute Ischemic Stroke. *The Izrael Medical Association*, November 2006, vol. 8, no. 11, pp. 788-792.

45. LEVITAN, I. B., KACZMAREK, L. K. *The Neuron - Cell and Molecular Biology*. 2nd Ed., NY and Oxford: Oxford University Press 1997, p. 543.

46. LESNEFSKY, E. J., HOPPEL, C. L. Ischemia-reperfusion injury in the aged heart: role of mitochondria. *Arch. Biochem. Biophys*, 2003, vol. 420, no. 2, pp. 287–297.

47. LODISH, H., et al. *Molecular Cell Biology.* [online]. © 2000 [cit. 2008-01-30]. URL: <http://www.ncbi.nlm.nih.gov/books/bv.fcgi?rid=mcb.TOC>

48. LUDWIN, S. K. The pathobiology of the oligodendrocyte. *Jounal of Neuropathology and Experimental Neurology* 1997, vol. 56, no. 2, pp. 111–124.

49. LYONS, S. A., et al. Distinct Physiologic Properties of Microglia and Blood-Borne Cells in Rat Brain Slices after Permanent Middle Cerebral Artery Occlusion. *Journal of Cerebral Blood Flow & Metabolism*, November 2000, vol. 20, no. 11, pp. 1537–1549.

50. MABUCHI, T., et. al. Contribution of microglia/macrophages to expansion of infarction and response of oligodendrocytes after focal cerebral ischemia in rats. *Stroke,* July 2000, vol. 31, no. 7, pp. 1735-1743.

51. MANNELLA, C. A., BUTTLE, K., RATH, B. K., MAKRO, M. Electron microscopic tomography of rat-liver mitochondria and their interaction with the endoplasmic reticulum. *Biofactors (Oxford, England)*, 1998, vol. 8, pp. 225–228.

52. MANNELLA, C. A., MAKRO, M., BUTTLE, K. Reconsidering mitochondrial structure: new views of an old organelle. *Trends Biochem. Sci*, 1997, vol. 22, pp. 37–38.

53. MARTIN, L. J., et al. Neurodegeneration in excitotoxicity, global cerebral ischemia, and target deprivation: a perspective on the contributions of apoptosis and necrosis. *Brain Research Bulletin*, July 1998, vol. 46, no. 4, pp. 281-309.

54. McCORMACK, J. G., HALESTRAP, A. P., DENTON, R. M., 1990. Role of calcium ions in regulation of mammalian intramitochondrial metabolism. *Physiol. Rev.*, 1990, vol. 70, no. 2, pp. 391–425.

55. MESSING, R. O. Nervous system disorders, In: *Pathophysiology of Disease: An Introduction to Clinical Medicine*, 4th ed. New York: Lange Medical Books/McGraw-Hill Medical Publishing Division 2003, pp. 143–188.

56. MIZUNO, Y., OHTA, S., TANAKA, M., TAKAMIYA, S., SUZUKI, K., SATO, T., OYA, H., OZAWA, T., KAGAWA, Y. Deficiencies in complex I subunits of the respiratory chain in Parkinson's disease. *Biochem. Biophys. Res. Commun*, 1989, vol. 163, no. 3, pp. 1450–1455.

57. MONTERO, M., ALONSO, M. T., ALBILLOIS, A., GAGSIA-SANCHO, J., ALVAREZ, J. Mitochondrial Ca^{2+} induced Ca^{2+} release mediated by the Ca^{2+} uniporter. *Mol. Biol. Cell.*, 2001, vol. 12, pp. 63–71.

58. NÄSLUND, J., HAROUTUNIAN, V., MOHS, R., DAVIS, K.-L., DAVIES, P., GREENGARD, P., BUXBAUM, J.-D. Correlation between elevated levels of amyloid b-peptide in the brain and cognitive decline. *Jama*, 2000, vol. 283, pp. 1571–1577.

59. NEWMAN, E. A. Glia and synaptic transmission. In: *Neuroglia*, 2nd edition, New York: Oxford University Press, 2004, Chapter 28, pp. 355-366.

60. NIEDERÖST, B., et al. Nogo-A and myelin-associated glycoprotein mediate neurite growth inhibition by antagonistic regulation of RhoA and Rac1. *The Journal of Neuroscience,* December 2002, vol. 22, no. 23, pp. 10368-10376.

61. NIEDERÖST, B. P., et al. Bovine CNS myelin contains neurite growth-inhibitory activity associated with chondroitin sulfate proteoglycan. *The Journal of Neuroscience,* October 1999, vol. 19, no. 20, pp. 8979-8989.

62. *NINDS Stroke Information Page.*[online] URL: < http://www.ninds.nih.gov/disorders/stroke/stroke.htm > [cit. 2008-02-11].

63. OERTLE T., et al. Nogo-A inhibits neurite outgrowth and cell spreading with three discrete regions. *The Journal of Neuroscience*, July 2003, vol. 23, no. 13, pp. 5393-5406.

64. O´MARA, S. The subiculum: what it does, what it might do, and what neuroanatomy has yet to tell us. *Journal of anatomy*, September 2005, vol. 207, no. 3, pp. 271-82.

65. OLAWALE, A. R., et al. Axonal Regeneration in the Peripheral Nervous System of Mammals. In: *Neuroglia*, 2nd edition, New York: Oxford University Press 2004, Chapter 36, pp. 454-466.

66. PANOV, A. V., GUTEKUNST, C. A., LEAVITT, B. R., HAYDN, M. R., BURKE, J. R., STRITTMATTER, W. J., GREENAMYRE, J. T. Early mitochondrial calcium defects in Huntington's disease are a direct effect of polyglutamines. *Nat. Neurosci.*, vol. 5, no. 8, pp. 731–736.

67. PAOLUCCI, S., et al. Early versus delayed inpatient stroke rehabilitation: A matched comparison conducted in Italy. *Archives of Physical Medicineand Rehabilitation*, June 2000, vol. 81, no. 6, pp. 695-700.

68. PAPADOPOULOS, C. M., et al. Dendritic plasticity in the adult rat following middle cerebral artery occlusion and Nogo-a neutralization. *Cerebral Cortex*, April 2006, vol. 16, no. 4, pp. 529–536.

69. PARKER Jr., W.D., BOYSON, S. J., PARKS, J. K. Abnormalities of the electron transport chain in idiopathic Parkinson's disease. *Ann. Neurol.*, 1989, vol. 26, no 6, pp 719–723.

70. PAXINOS, G., WATSON, C. *The Rat Brain in Stereotaxic Coordinates*, 4th edition, San Diego: Elsevier Academic Press, 1998. 117 figures.

71. PAXINOS, G., WATSON, C. *The Rat Brain in Stereotaxic Coordinates* [CD-ROM]. San Diego: Elsevier Academic Press,1998.

72. PFEIFFER, S. E., WARRINGTON, A. E., BANSAL, R. The oligodendrocyte and its many cellular processes. *Trends in Cell Biology*, June 1993, vol. 3, no. 6, pp. 191-197.

73. PRALONG, W. F., HUNYADY, L., VARNAI, P., WOLLHEIM, C. B., SPAT, A. Pyridine nucleotide redox state parallels production of aldosterone in potassium-stimulated adrenal glomerulosa cells. *Proc. Natl. Acad. Sci. USA*, vol. 89, no. 1, pp 132–136.

74. RANSOM, B. R., YE, Z. - C., Gap Junctions and Hemichanels , In: *Neuroglia*, 2nd edition. New York: Oxford University Press 2004, Chapter 13, pp 177-189.

75. RIZZUTO, R., DUCHEN, M. R., POZZAN, T. Flirting in little space: the ER/mitochondria Ca^{2+} liaison. Sci. STKE, 2004, p. 215.

76. RHAWN, J. *Neocortex*. [online]. © 2000-2006 [cit. 2008-02-05]. URL: <http://brainmind.com/Neocortex.html>

77. ROSAMOND W., et al. Heart disease and stroke statistics–2007 update: a report from the American Heart Association Statistics Committee and Stroke Statistics Subcommittee. *Circulation*, February 2007, vol. 115, no. 5, pp. 69 – 171.

78. ROSAMOND, W. D., et al. Stroke incidence and survival among middle-aged adults: 9-year follow-up of the Atherosclerosis Risk in Communities (ARIC) cohort. *Stroke*, April 1999, vol. 30, no. 4, pp. 736 –743.

79. SACCO, R. L., et al. Stroke incidence among white, black, and Hispanic residents of an urban community: the Northern Manhattan Stroke Study. *American Journal of Epidemiology,* February 1998, vol. 147, no. 3, pp. 259 – 268.

80. SAMSA, G. P., et al. Utilities for major stroke: results from a survey of preferences among persons at increased risk for stroke. *American Heart Journal*, October 1998, vol. 136, pp. 703–713.

81. SCHAPIRA, A. H., COOPER, J. M., DEXTER, D., JENNER, P., CLARK, J. B., MARSDEN, C. D. Mitochondrial complex I deficiency in Parkinson's disease. *Lancet*, 1989, 1 (8649), 1269.

82. SCHUBERT, D., PIASECKI, D. Oxidative glutamate toxicity can be a component of the excitotoxicity cascade. *J. Neurosci.*, 2001, vol. 21, no 19, pp 7455–7462.

83. SHERER, T. B., BETARBET, R., S´TOUT, A. K., LUND, S., BAPTITSTA, M., PANOV, A. V., COOKSON, M. R., GREENAMYRE, J. T. An in vitro model of Parkinson's disease: linking mitochondrial impairment to altered alpha-synuclein metabolism and oxidative damage. *J. Neurosci.*, 2002, vol. 22, no 16, pp. 7006–70015.

84. SHERER, T.B., BEATBERT, R., TESTA, C. M., SEO, B. B., RICHARDSON, J. R., KIM, J. H., MILLER, G. W., YAGI, T., MATSUNO-YAGI, A., GREENAMYRE, J.T. Mechanism of toxicity in rotenone models of Parkinson's disease. *J. Neurosci.*, 2003, vol. 23, no. 34, pp. 10756–10764.

85. SHIINO, A., MATSUDA, M., HANDA, J., CHANCE, B. Poor recovery of mitochondrial redox state in CA1 after transient forebrain ischemia in gerbils. *Stroke*, November 1998, vol. 29, no. 11, pp. 2421-2425.

86. STEGMAYR, B., et al. Stroke incidence and mortality correlated to stroke risk factors in the WHO MONICA Project. An ecological study of 18 populations. *Stroke*, July 1997, vol. 28, no. 7, pp.1367-1374.

87. STEINMETZ, M., et al. Chronic enhancement of the intrinsic growth capacity of sensory neurons combined with the degradation of inhibitory proteoglycans allows functional regeneration of sensory axons through the dorsal root entry zone in the mammalian spinal cord. *The Journal of Neuroscience*, August 2005, vol. 25, no. 35, pp. 8066-8076.

88. TANG, Y., ZUCKER, R. S. Mitochondrial involvement in post-tetanic potentiation of synaptic transmission. *Neuron*, 1997, vol. 18, pp. 483–491.

89. THAYER, S. A., MILLER, R. J. Regulation of the intracellular free calcium concentration in single rat dorsal root ganglion neurones in vitro. *J. Physiol.*, 1990, vol. 425, pp. 85–115.

90. TONG, W. Traumatic Brain Injury in the Immature Mouse Brain: Characterization of Regional Vulnerability. *Experimental Neurology*, July 2002, vol. 176, no. 1, pp. 105-116.

91. TREVOR, H., PARIS, M. D. Stroke Rehabilitation *Northeast Florida Medicine Journal*, Summer 2007, vol. 58, no. 2, pp. 26-30.

92. TUDNER, D. A., FOSTER, K. A., GALEFFI, F., SOMJEN, G. G. Differences in O_2 availability resolve the apparent discrepancies in metabolic intrinsic optical signals in vivo and in vitro. *Trends in Neurosciences*, August 2007, vol 30, no. 8, pp. 390-398.

93. VALERIANI, V., DEWAR, D., McCULLOCH, J. Quantitative assessment of ischemic pathology in axons, oligodendrocytes, and neurons: Attenuation of damage after transient ischemia. *Journal of Cerebral Blood Flow and Metabolism*, May 2000, vol. 20, no. 5, pp. 765-771.

94. VOURC'H, P., ANDRES, C. Oligodendrocyte myelin glycoprotein (OMgp): evolution, structure and function. *Brain Research Reviews*, May 2004, vol. 45, no. 2, pp. 115-124.

95. WATTS, J., THOMSON, A. M. Excitatory and inhibitory connections show selectivity in the neocortex- Symposium report. *The Journal of Physiology*, January 2005, vol. 562, part 1, pp. 89-97.

96. WELLS, R. B. *Cortical Neurons and Circuits: A Tutorial Introduction* [online]. © 2005 [cit. 2008-02-05]. URL: <http://www.mrc.uidaho.edu/~rwells/techdocs/Cortical%20Neurons%20and%20Circuits.pdf>

97. WITTNER, L., et al. Three-dimensional reconstruction of the axon arbor of a CA3 pyramidal cell recorded and filled in vivo *Brain Structure and Function*, July 2007, vol. 212, no. 1, pp. 75-83.

98. ZORATTI, M., SZABO, I. The mitochondrial permeability transition. *Biochim. Biophys. Acta*, 1995, vol. 1241, no. 2, pp. 139–176.

10. ATTACHMENTS

Attachment No. 1

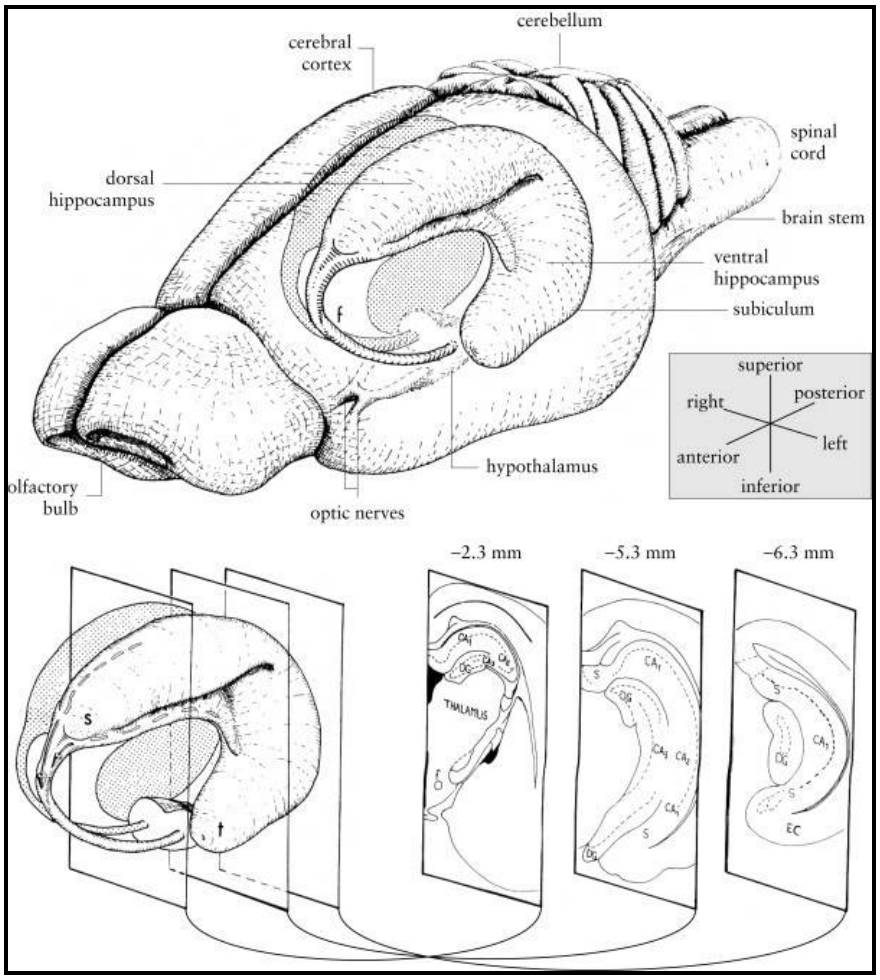

Diagram of the rat hippocampus. Drawings of the rat brain showing the three-dimensional organization of the hippocampus and related structures. Three coronal sections through the left hippocampus are shown at the bottom right of the figure, with their approximate anteroposterior coordinate relative to bregma. CA1, CA2, CA3: cornu ammonis fields 1–3; DG: dentate gyrus; EC: entorhinal cortex; f: fornix; s: septal pole of the hippocampus; S: subiculum; t: temporal pole of the hippocampus. (1)

Attachment No. 2

The statistic data evaluation using the software Sigma Stat version 3.5, Systat software Inc., descriptive statistics and paired t-test were performed to evaluate the temperature dependency (26°C/36°C) of FAD signal maximal values at 2T stimulus intensity:

Paired t-test: Monday, September 01, 2008, 9:12:40

Data source: Data 1 in Notebook 1

Normality Test: Passed (P = 0,788)

Treatment Name	N	Missing	Mean	Std Dev	SEM
2T 26°C	14	0	2,146	1,406	0,376
2T 36°C	14	0	1,713	0,893	0,239
Difference	14	0	0,434	1,570	0,419

t = 1,034 with 13 degrees of freedom. (P = 0,320)

95 percent confidence interval for difference of means: -0,473 to 1,340

The change that occurred with the treatment is not great enough to exclude the possibility that the difference is due to chance (P = 0,320)

Power of performed test with alpha = 0,050: 0,055

The power of the performed test (0,055) is below the desired power of 0,800

Less than desired power indicates you are less likely to detect a difference when one actually exists. Negative results should be interpreted cautiously.

Attachment No. 3

The statistic data evaluation using the software Sigma Stat version 3.5, Systat software Inc., descriptive statistics and paired t-test were performed to evaluate the temperature dependency (26°C/36°C) of FAD signal maximal values at 3T stimulus intensity:

Paired t-test: Monday, September 01, 2008, 9:13:18

Data source: Data 1 in Notebook 1

Normality Test: Passed (P = 0,140)

Treatment Name	N	Missing	Mean	Std Dev	SEM
3T 26°C	22	0	2,704	1,369	0,292
3T 36°C	22	0	1,515	0,664	0,142
Difference	22	0	1,188	1,055	0,225

t = 5,285 with 21 degrees of freedom. (P = <0,001)

95 percent confidence interval for difference of means: 0,721 to 1,656

The change that occurred with the treatment is greater than would be expected by chance; there is a statistically significant change (P = <0,001)

Power of performed test with alpha = 0,050: 1,000

Attachment No. 4

The statistic data evaluation using the software Sigma Stat version 3.5, Systat software Inc., descriptive statistics and paired t-test were performed to evaluate the temperature dependency (26°C/36°C) of FAD signal maximal values at 4T stimulus intensity:

Paired t-test Monday, September 01, 2008, 9:13:56

Data source: Data 1 in Notebook 1

Normality Test: Passed (P = 0,098)

Treatment Name	N	Missing	Mean	Std Dev	SEM
4T 26°C	12	0	2,299	0,582	0,168
4T 36°C	12	0	1,353	0,369	0,107
Difference	12	0	0,946	0,771	0,223

t = 4,251 with 11 degrees of freedom. (P = 0,001)

95 percent confidence interval for difference of means: 0,456 to 1,436

The change that occurred with the treatment is greater than would be expected by chance; there is a statistically significant change (P = 0,001)

Power of performed test with alpha = 0,050: 0,972

Attachment No. 5

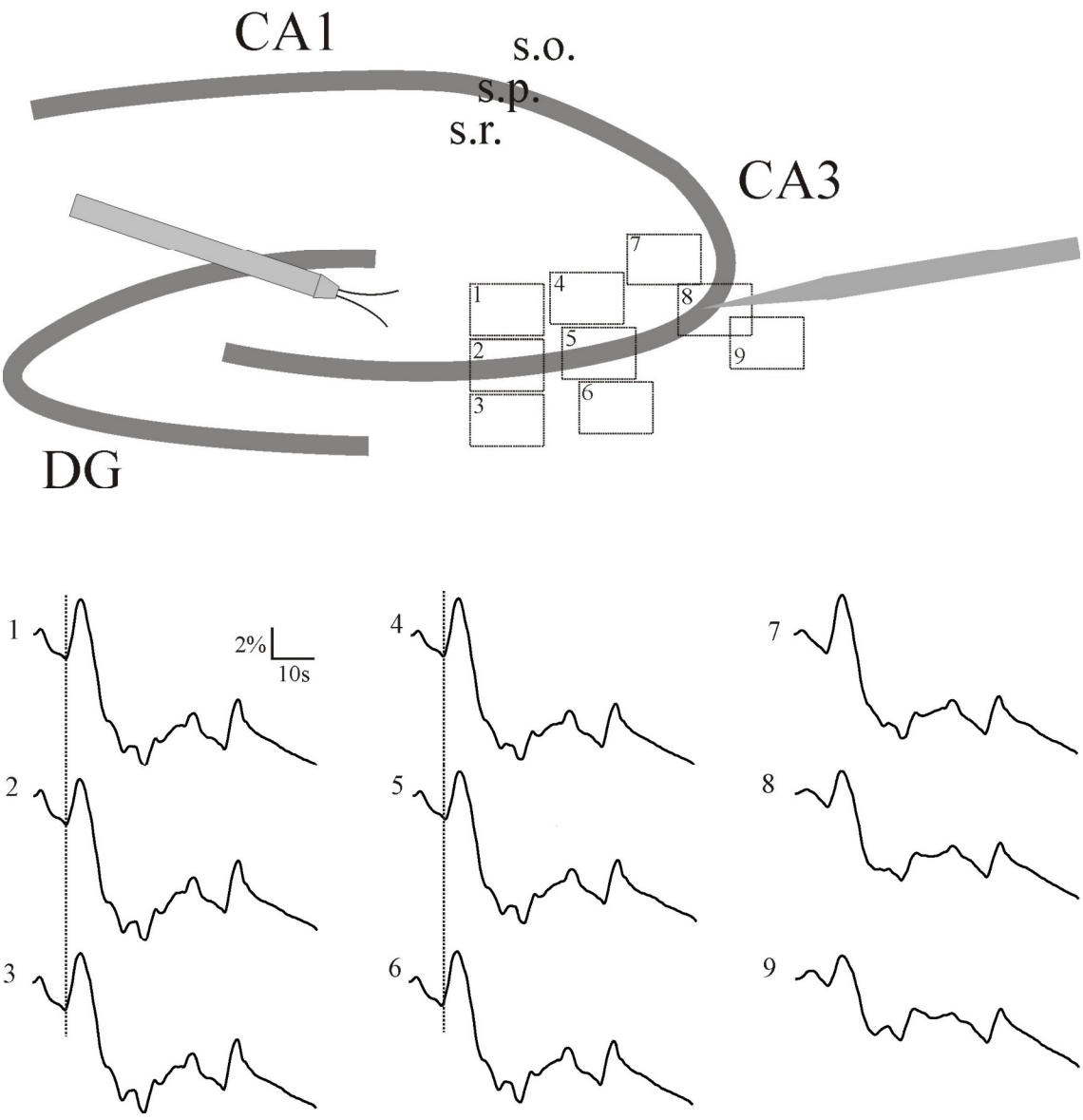

Diagram of 9 different ROIs in one slice trying to show 3 FAD signals from *stratum radiale*, 3 from *stratum pyramidale* and 3 from *stratum oriens*. The ROIs were placed so, that they formed 3 columns – each column containing 1 ROI from different layer. The columns included all layers at different distances (300 um, 600um, 900 um) from the stimulating electrode. FAD signal could be evaluated in the certain distance from the electrode and compared the different layers. Diagrams of FAD signals curves in time from each ROI are shown schematically bellow.
Abbreviations: CA = cornu ammonis; DG = dentate gyrus; s.o. = stratum oriens; s.p. = stratum pyramidale; s.r. = stratum radiale.